AD_____

Award Number: DAMD17-99-1-9407

TITLE: IGF-IR, Cell Adhesion and Metastasis

PRINCIPAL INVESTIGATOR: Eva Surmacz, Ph.D.

CONTRACTING ORGANIZATION: Thomas Jefferson University
Philadelphia, Pennsylvania 19107

REPORT DATE: September 2001

TYPE OF REPORT: Annual

PREPARED FOR: U.S. Army Medical Research and Materiel Command
Fort Detrick, Maryland 21702-5012

DISTRIBUTION STATEMENT: Approved for Public Release;
Distribution Unlimited

REPORT DOCUMENTATION PAGE

Form Approved
OMB No. 074-0188

1. AGENCY USE ONLY (Leave blank)	2. REPORT DATE	3. REPORT TYPE AND DATES COVERED
	September 2001	Annual (15 Aug 00 - 14 Aug 01)

4. TITLE AND SUBTITLE
IGF-IR, Cell Adhesion and Metastasis

5. FUNDING NUMBERS
DAMD17-99-1-9407

6. AUTHOR(S)
Eva Surmacz, Ph.D.

7. PERFORMING ORGANIZATION NAME(S) AND ADDRESS(ES)
Thomas Jefferson University
Philadelphia, Pennsylvania 19107

E-Mail: Eva.Surmacz@mail.tju.edu

8. PERFORMING ORGANIZATION REPORT NUMBER

9. SPONSORING / MONITORING AGENCY NAME(S) AND ADDRESS(ES)
U.S. Army Medical Research and Materiel Command
Fort Detrick, Maryland 21702-5012

10. SPONSORING / MONITORING AGENCY REPORT NUMBER

11. SUPPLEMENTARY NOTES

12a. DISTRIBUTION / AVAILABILITY STATEMENT
Approved for Public Release; Distribution Unlimited

12b. DISTRIBUTION CODE

13. Abstract *(Maximum 200 Words)* *(abstract should contain no proprietary or confidential information)*

The insulin-like growth factor I receptor (IGF-IR) is a multifunctional tyrosine kinase that has been implicated in breast cancer. Current evidence suggests an important role of the IGF-IR in the growth and survival of ER-positive primary breast tumors. However, the function of the IGF-IR in breast cancer metastasis is unknown. Previously we have shown that IGF-I induces cell-cell adhesion in breast cancer cells. Consequently, we proposed to investigate the molecular mechanism of IGF-IR-stimulated cell adhesion, and the role of IGF-IR overexpression in breast cancer metastasis.

We demonstrated that the IGF-IR promotes cell-cell adhesion through the E-cadherin (E-cad)-complex. The effects of the IGF-IR depend on tyrosine kinase activity of the receptor and require the expression of a junction protein ZO-1. The IGF-IR, however, does not influence the levels or phosphorylation status of E-cad, alpha-, beta-, and gamma-catenins. In experimental metastasis model, E-cad-positive cells overexpressing the IGF-R have reduced metastatic potential.

14. Subject Terms (keywords previously assigned to proposal abstract or terms which apply to this award)
Breast cancer, Insulin-Like Growth factor, Cell-Cell Adhesion, Motility

15. NUMBER OF PAGES
47

16. PRICE CODE

17. SECURITY CLASSIFICATION OF REPORT	18. SECURITY CLASSIFICATION OF THIS PAGE	19. SECURITY CLASSIFICATION OF ABSTRACT	20. LIMITATION OF ABSTRACT
Unclassified	Unclassified	Unclassified	Unlimited

TABLE OF CONTENTS

INTRODUCTION

The insulin-like growth factor I (IGF-I) receptor (IGF-IR) is a ubiquitous multifunctional tyrosine kinase. The IGF-IR regulates normal breast development; however, hyperactivation of the same receptor has been implicated in breast cancer (1). In particular, overexpression of either the IGF-IR or its major signaling substrate IRS-1 in estrogen receptor (ER)-positive breast tumors has been linked with cancer recurrence at the primary site. Furthermore, high circulating levels of IGF-I (an IGF-IR ligand) have been associated with increased breast cancer risk in premenopausal women (1).

Although current evidence suggests that abnormal activation of the IGF-IR may contribute to the autonomous growth and increased survival of primary ER-positive breast tumors, the function of this receptor in breast cancer metastasis is not clear. For instance, some small clinical studies demonstrated a correlation between IGF-IR expression in node-positive tumors and worse prognosis. Other data linked IGF-IR expression with better clinical outcome, as the IGF-IR was predominantly expressed in a subset of breast tumors with good prognostic characteristics (1). In the experimental setting, anti-IGF-IR strategies were successfully applied to inhibit the growth and spread of human breast cancer xenografts, which implicated the IGF-IR in metastasis (1). Thus, understanding whether hyperactivation of the IGF-IR is a factor promoting breast cancer metastasis is of great importance.

Our previous data demonstrated that overexpressed IGF-IRs not only promote breast cancer cells growth, but also activate aggregation and prolong survival of detached cells (2). This process was blocked with a specific antibody against E-cadherin (E-cad)—a major cell-cell adhesion protein expressed by epithelial cells, suggesting that the E-cad complex mediates IGF-IR effects. The molecular mechanism of IGF-I-induced E-cad-dependent adhesion and the significance in the process of metastasis have been unknown. Consequently, our goal was to study the effects of IGF-I on the expression of E-cad and E-cad-associated proteins, to determine the interactions of the IGF-IR with these adhesion proteins, and to evaluate the importance of the IGF-IR/E-cad interactions in metastasis in vivo. In parallel, we addressed the function of the IGF-IR in metastatic breast cancer cells that have lost E-cad expression.

TECHNICAL REPORT

During this reporting performance period (Year 2) we continued the projects initiated in Year 1. The research proceeded according to the SOW.

Project I: IGF-IR interactions with the E-cad complex.

The proposal was based on our previous observation that MCF-7 breast cancer cells overexpressing the IGF-IR exhibit increased aggregation in 3-dimensional (3-D) culture. Our results in Year 1 implicated that IGF-IR-induced adhesion is mediated through the E-cad complex. We studied whether overexpression of the IGF-IR in MCF-7 cells can modulate the levels of E-cad and associated adhesion proteins. We found that the levels of E-cad, alpha-, and beta-catenin were not affected by IGF-IR overexpression. However, the levels of ZO-1, a scaffolding protein linking E-cadherin through alpha-catenin to the actin cytoskeleton (3, 4), were significantly increased in cells overexpressing the IGF-IR (MCF-7/IGF-IR clones 17, 15, and 12) *(Fig. 2, .Mauro et al., Appendix).* Subsequent experiments demonstrated that ZO-1

mRNA was overexpressed in MCF-7/IGF-IR cells relative to MCF-7 cells *(Fig. 4, Mauro et al,. Appendix)*. The analysis of interactions of the IGF-IR with adhesion proteins revealed that the IGF-IR co-precipitates with E-cadherin and ZO-1 *(Fig. 5, Mauro et al.,Appendix)*. The amounts of the IGF-IR found in E-cad and ZO-1 immunoprecipitates were greater in IGF-IR overexpressing cells *(Fig. 5, Mauro et al,. Appendix)*. IGF-IR and ZO-1 also associated with alpha-catenin, with greater amounts of these complexes found in MCF-7/IGF-IR cells *(Fig. 5, Mauro et al., Appendix)*. In addition, we noted greater binding of ZO-1 to actin in MCF-7/IGF-IR cells *(Fig. 5, Mauro et al., Appendix)*. This all suggested that the mechanism by which the IGF-IR stimulates adhesion depends on ZO-1 *(Fig. 6, Mauro et al., Appendix)*.

In Year 2, we confirmed that the E-cad complex is necessary to mediate cell-cell adhesion induced by the IGF-IR. Using MDA-MB-231 E-cad-negative cells, we created cell line overexpressing the IGF-IR, MDA-MB-231/IGF-IR cells. In MDA-MB-231/IGF-IR cells, high levels of the IGF-IR did not stimulate aggregation, whereas similar expression of the IGF-IR in MCF-7 E-cad positive cells induced adhesion. However, when E-cad was re-expressed in MDA-MB-231/IGF-IR cells, cell-cell adhesion was restored *(Fig. 1, Mauro et al., Appendix)*.

To confirm our previous observation that ZO-1 expression is necessary for cell-cell adhesion induced by the IGF-IR, we employed anti-ZO-1 antisense strategy. We developed anti-ZO-1 antisense RNA construct and subsequently we created, by stable transfection, MCF-7/IGF-IR/anti-ZO-1 cell lines. In these clones, the levels of ZO-1 were downregulated, whereas the expressions of E-cad and IGF-IR were unchanged. The lower levels of ZO-1 in MCF-7/IGF-IR/antti-ZO-1 cells coincided with reduced cell-cell adhesion *(Fig.7, Mauro et al., Appendix)*.

We also addressed the role of IGF-IR tyrosine kinase activity in the regulation of cell-cell adhesion. We developed MCF-7 cells expressing dominant-negative kinase "dead" IGF-IR by stable transfection. The IGF-IR signaling was inhibited in these cells and this inhibition was paralleled by decreased cell-cell adhesion and lower basal expression of ZO-1. To avoid clonal variability problem, the "dead" IGF-IR was also expressed in MCF-7 cells by efficient transient transfection with Fugene 6. The results obtained with the individual clones were confirmed using the mixed population of transfected cells *(Fig. 3, Mauro et al., Appendix)*.

All above data and technology are described in detail in the manuscript by Mauro, L., Bartucci, M., Morelli, C., Ando', S., and Surmacz, E. IGF-I receptor-induced cell-cell adhesion of MCF-7 breast cancer cells requires the expression of a junction protein ZO-1, in revision, J. Biol. Chem. (Appendix).

The IGF-IR/E-cad interaction in vivo. We obtained preliminary data on the metastatic potential of MCF-7/IGF-IR cells. It is well established that MCF-7 cells injected directly into circulation produce radiographically detectable osteolytic/osteosclerotic bone metastasis in 10-15 weeks (5). In collaboration with Dr. T. Yoneda (University of Texas, San Antonio), we obtained data suggesting that overexpression of IGF-IR in MCF-7 cells significantly attenuated (~ 10-fold) their ability to metastasize to bone. Specifically, MCF-7 cells and MCF-7/IGF-IR clone 15 ($5x10^5$ cells) were inoculated into the left cardiac ventricle in 4-week old female nude mice. 15 weeks after the inoculation, the mice were sacrificed and bone metastases were analyzed by X-ray. MCF-7 cells produced 0.576 (SE 0.116) mm^2 bone metastases, whereas MCF-7/IGF-IR produced 0.0522 (SE 0.0331) mm^2 metastases. These results confirm our observations in vitro and indicate that IGF-IR may play a negative role in the dissemination of breast cells.

Project II: IGF-IR function in E-cadherin-negative cells.

Using MDA-MB-231 cells, a well-described metastatic cell line lacking E-cad expression, we generated several clones expressing different levels of the IGF-IR (Year 1 of this project*)(Fig. 1, Bartucci et al., Appendix).* IGF-IR overexpression in E-cad negative cells did not stimulate cell-cell adhesion (see above). We asked, therefore, what is the function of the IGF-IR in these cells. We found that IGF-I was not a mitogen or a survival factor for these ER-negative metastatic cells, whereas the same factor exerted growth-promoting and anti-apoptotic action in ER-positive MCF-7 cells *(Tab. 1 and Fig. 2 and 3, Bartucci et al., Appendix).* Notably, the lack of growth-related properties of IGF-I in MDA-MB-231 cells was evident in all clones derived from this cell line, regardless of IGF-IR expression levels. To investigate why the IGF-IR was not inducing mitogenic signals in MDA-MB-231 cells, we studied IGF-IR activation and intracellular signaling. We focused on two IGF-IR pathways known to control growth and survival of ER-positive breast cancer cells, namely IGF-IR/IRS-1/PI-3K/Akt and MAPK pathways (1). We found that in MDA-MB-231 cells, the IGF-IR/IRS-1 signal was normal, however the cells were not able to sustain the downstream PI-3K/Akt activation. We hypothesized that this feature may contribute to the lack of mitogenic/survival response to IGF in metastatic cells *(Fig. 4, 5,and 6, Bartucci et al., Appendix).*

Considering that the IGF-IR was not mitogenic in ER-negative cells, we asked whether this receptor could transmit other signals critical for tumor progression. We focused on growth-unrelated functions such as adhesion and migration. We found that unlike with growth and survival, the IGF-IR was able to induce migration in MDA-MB-231 cells and MDA-MB-231/IGF-IR clones. The induction of migration was proportional to the levels of the IGF-IR *(Tab.3, Bartucci et al., Appendix).* The manuscript describing these findings was submitted in August 2000.

In Year 2, we performed several experiments requested by the reviewers of the submitted manuscript to better delineate the pathways by which IGF-I stimulates cell migration. The experiments with specific inhibitors suggested that IGF-I-induced migration was transmitted through p38 kinase and PI-3 kinase pathways and inhibited by ERK1/2 MAP kinases *(Tab. 4, Bartucci et al., Appendix).* In a control experiment, we demonstrated that the compounds used indeed blocked IGF-I signal transmission through the target pathways *(Fig.7, Bartucci et al., Appendix).*

To ascertain that kinase inhibitors blocked only cell migration without affecting cell growth or survival, we studied the cells at 4, 8, 12, and 24 h of the treatment. At these time points, the inhibitors of ERK1/2 and p38 did not affect cell growth/survival, but the inhibitor of PI-3K reduced cell number at 24h. Therefore the treatment with the PI-3K inhibitor was carried out for 12h, when no effects on cell growth/survival were noted, but the migration was blocked. *(Tab.4 , Bartucci et al., Appendix).*

We also performed control experiments in which cell lines transfected with the empty vectors were studied. These experiments were done to ascertain that the observed differences in MDA-MB-231/IGF-IR and MCF-7/IGF-IR cells were due to the expression of the transfected IGF-IR and not a result of a clonal variation. *(Fig.2, and 3, and Tab3, Bartucci et al., Appendix).*

Key Research Accomplishments:

- Demonstrated that the activation or overexpression of the IGF-IR induces cell-cell adhesion in E-cad-positive but not in E-cad-negative cells. IGF-IR-mediated cell-cell adhesion in E-cad-positive cells requires tyrosine kinase activity of the IGF-IR and depends on cellular expression of a junction protein, ZO-1.

- Demonstrated, using intracardiac injection model, that overexpression of the IGF-IR reduces metastatic potential of E-cad-positive cells tested in vivo.

- Demonstrated that activation of the IGF-IR in E-cadherin-negative ZO-1-negative MDA-MB-231 cells does not induce cell-cell adhesion, but it regulates cell migration through p38 kinase and PI-3K pathways.

Reportable Outcomes:

1. Manuscripts, abstracts and scientific presentations:

Manuscripts:

1. Bartucci, M., Morelli, C., Mauro, L., Ando', S., Surmacz, E. Differential insulin-like growth factor I receptor signaling and function in estrogen receptor (ER)-positive MCF-7 and ER-negative MDA-MB-231 breast cancer cells. Cancer Research 61: 2001.

2. Mauro, L., Bartucci, M., Morelli, C., Ando', S., Surmacz, E. IGF-I receptor-induced cell-cell adhesion of MCF-7 breast cancer cells requires the expression of a junction protein ZO-1, in revision, J. Biol. Chem.

Abstracts (Oral Presentations):

Salerno, M., Mauro, L., Panno, M. L., Belizzi, D., Sisci, D., Miglietta, A., Surmacz, E., Ando', S. Estradiol enhance IRS-1 gene expression and amplifies insulin signaling in ER-positive breast cancer cells. The Endocrine Society 83rd Annual Meeting. Denver, Co, June 20-23, 2001.

Invited Talks:

Surmacz, E. Is IGF-IR involved in breast cancer? Oncology Group Meeting. Thomas Jefferson University, Philadelphia, Pa, June 28, 2001.

Surmacz, E. Differential IGF-I signaling in ER-positive and ER-negative breast cancer cells. Department of Radiology. University of Pennsylvania, Philadelphia, PA, May 16, 2001.

Surmacz, E. IGF signaling in ER-negative breast cancer cells. Postgraduate School in Molecular Pathology. University of Calabria, Italy, May 11, 2001.

Surmacz, E. IGF-I receptor/estrogen receptor cross-talk in breast cancer. Postgraduate School in Molecular Pathology. University of Calabria, Italy, May 10, 2001.

Surmacz, E. Differential IGF-I receptor signaling in ER-positive and ER-negative breast cancer cells. Kimmel cancer Center, Staff Seminar Series, Philadelphia, PA, April 9, 2001.

Surmacz, E. Differential IGF-I receptor signaling in ER-positive and ER-negative breast cancer cells. Temple University, Center for Neurovirology and Tumor Biology, Philadelphia, PA, April 5, 2001.

Surmacz, E. Role of the E-cadherin complex in breast cancer cell adhesion. Philadelphia Cadherin Club Meeting. Lankenau Cancer Research Center, Wynnewood, PA, March 1, 2001.

Surmacz, E. Differential IGF-IR function in ER-positive and ER-negative breast cancer cells. Astra Zeneca, Macclesfield, U.K., September 18, 2000.

Surmacz, E. Evolution of IGF-IR signaling during breast cancer progression. "IGFs and Cancer" International Symposium, Halle, Germany, September 14-17, 2000.

2. Patents and licenses: None

3. Degrees: N/A

4. Development of biologic reagents:

- MCF-7/IGF-IR cells expressing antisense ZO-1 RNA

5. Databases: None

6. Funding applied for:

2001/2002, AstraZeneca, U.K. Research Grant "Mechanisms of IGF-I Receptor-Mediated Migration and Invasion in Breast Cancer Cells", $50,000 direct costs, funded

7. Employment applied for: None

Conclusions

The IGF-IR regulates cell-cell adhesion in ER-positive cells. The mechanism of this phenomenon requires tyrosine kinase activity of the IGF-IR and involves overexpression of a junction protein—ZO-1.

The IGF-IR has different functions in E-cad-negative cells, where it does not induce cell-cell adhesion, but stimulates cell migration.

References

1. Surmacz, E. Function of the IGF-IR in breast cancer. J. Mammary Gland Biol. Neopl., 5: 95-105, 2000.

1. Guvakova, M. A., and Surmacz, E. Overexpressed IGF-I receptors reduce estrogen growth requirements, enhance survival and promote cell-cell adhesion in human breast cancer cells. Exp. Cell Res., 231: 149-162, 1997.

3. Rajasekaran, A.K., Hojo, M., Huima, T., Rodriguez-Boulan, E. Catenins and zonula occludens-1 form a complex during early stages in the assembly of tight junctions. J. Cell Biol. 132: 451-463, 1996.

4. Itoh, M., Nagafuchi, A., Moroi, S., Tsukita, S. Involvement of ZO-1 in cadherin-based cell adhesion through its direct binding to alpha catenin and actin filaments. J. Cell Biol. 138: 181-192, 1997.

5.Yoneda, T., Sasaki, A., Mundy, G. R. Osteolytic bone metastasis in breast cancer. Breast Cancer Res. Treat. 32: 73-84, 1994.

[CANCER RESEARCH 61, ●●-●●●, September 15, 2001]

Differential Insulin-like Growth Factor I Receptor Signaling and Function in Estrogen Receptor (ER)-positive MCF-7 and ER-negative MDA-MB-231 Breast Cancer Cells[1]

Monica Bartucci, Catia Morelli, Loredana Mauro, Sebastiano Ando', and Eva Surmacz[2]

Kimmel Cancer Center, Thomas Jefferson University, Philadelphia, Pennsylvania 19107 [M. B., C. M., L. M., E. S.], and Department of Cellular Biology, University of Calabria, Calabria, Italy [M. B., C. M., L. M., S. A.]

AQ: A

87036

ABSTRACT

Fn1 Fn2 **The insulin-like growth factor I receptor (IGF-IR) is a ubiquitous and multifunctional tyrosine kinase that has been implicated in breast cancer development. In estrogen receptor (ER)-positive breast tumors, the levels of the IGF-IR and its substrate, insulin-receptor substrate 1 (IRS-1), are often elevated, and these characteristics have been linked with increased radioresistance and cancer recurrence. *In vitro*, activation of the IGF-IR/IRS-1 pathway in ER-positive cells improves growth and counteracts apoptosis induced by anticancer treatments. The function of the IGF-IR in hormone-independent breast cancer is not clear. ER-negative breast cancer cells often express low levels of the IGF-IR and fail to respond to IGF-I with mitogenesis. On the other hand, anti-IGF-IR strategies effectively reduced metastatic potential of different ER-negative cell lines, suggesting a role of this receptor in late stages of the disease.**

Here we examined IGF-IR signaling and function in ER-negative MDA-MB-231 breast cancer cells and their IGF-IR-overexpressing derivatives. We demonstrated that IGF-I acts as a chemoattractant for these cells. The extent of IGF-I-induced migration reflected IGF-IR levels and required the activation of phosphatidylinositol 3-kinase (PI-3K) and p38 kinases. The same pathways promoted IGF-I-dependent motility in ER-positive MCF-7 cells. In contrast with the positive effects on cell migration, IGF-I was unable to stimulate growth or improve survival in MDA-MB-231 cells, whereas it induced mitogenic and antiapoptotic effects in MCF-7 cells. Moreover, IGF-I partially restored growth in ER-positive cells treated with PI-3K and ERK1/ERK2 inhibitors, whereas it had no protective effects in ER-negative cells. The impaired IGF-I growth response of ER-negative cells was not caused by a low IGF-IR expression, defective IGF-IR tyrosine phosphorylation, or improper tyrosine phosphorylation of IRS-1. Also, the acute (15-min) IGF-I activation of PI-3 and Akt kinases was similar in ER-negative and ER-positive cells. However, a chronic (2-day) IGF-I exposure induced the PI-3K/Akt pathway only in MCF-7 cells. The reactivation of this pathway in ER-negative cells by overexpression of constitutively active Akt mutants was not sufficient to significantly improve proliferation or survival (with or without IGF-I), which indicated that other pathways are also required to support these functions.

Our results suggest that in breast cancer cells, IGF-IR can control nonmitogenic processes regardless of the ER status, whereas IGF-IR growth-related functions may depend on ER expression.

INTRODUCTION

Fn3 The IGF-IR[3] is a ubiquitous, transmembrane tyrosine kinase that has been implicated in different growth-related and growth-unrelated processes critical for the development and progression of malignant tumors, such as proliferation, survival, and anchorage-independent growth, as well as cell adhesion, migration, and invasion (1, 2).

The IGF-IR is necessary for normal breast biology, but recent clinical and experimental data strongly suggest that the same receptor is involved in the development of breast cancer (1, 3). The IGF-IR is overexpressed (up to 14-fold) in ER-positive breast cancer cells compared with its levels in normal epithelial cells (1, 4, 5). The elevated expression and hyperactivation of the IGF-IR has been linked with increased radioresistance and cancer recurrence at the primary site (4). Similarly, high levels of IRS-1, a major signaling molecule of the IGF-IR, correlated with tumor size and shorter disease-free survival in ER-positive tumors (6, 7).

IGF-IR ligands, IGF-I and IGF-II, are strong mitogens for many hormone-dependent breast cancer cell lines and have been found in the epithelial and/or stromal component of breast tumors (1). Importantly, higher levels of circulating IGF-I predict increased breast cancer risk in premenopausal women (8). *In vitro*, activation of the IGF-IR, especially the IGF-IR/IRS-1/PI-3K pathway in ER-positive breast cancer cells, counteracts apoptosis induced by different anticancer treatments or low concentrations of hormones (1, 9–11). On the other hand, overexpression of either the IGF-IR or IRS-1 in ER-positive breast cancer cells improves responsiveness to IGF and, in consequence, results in estrogen-independent proliferation (1, 12, 13). In agreement with these observations, blockade of IGF-IR activity with various reagents targeting the IGF-IR or its signaling through IRS-1/PI-3K reduced the growth of breast cancer cells *in vitro* and/or *in vivo* (1, 12, 14–17).

The requirement for the IGF-IR/IRS-1 pathway for growth and survival appears to be a characteristic of ER-positive, more differentiated, breast cancer cells. By contrast, ER-negative tumors and cell lines, often exhibiting less differentiated, mesenchymal phenotypes, express low levels of the IGF-IR and often decreased levels of IRS-1 (1, 17, 18). Notably, these cells do not respond to IGF-I with growth (1, 19–22). Despite the lack of IGF-I mitogenic response, the metastatic potential of ER-negative breast cancer cells can be effectively inhibited by different compounds targeting the IGF-IR. For instance, blockade of the IGF-IR in MDA-MB-231 cells by an anti-IGF-IR antibody reduced migration *in vitro* and tumorigenesis *in vivo*, and expression of a soluble IGF-IR in MDA-MB-435 cells inhibited adhesion on the extracellular matrix and impaired metastasis in animals (14, 16, 23). These observations suggested that in ER-negative cells, some functions of the IGF-IR must be critical for metastatic cell spread. Here we addressed the possibility that in ER-negative cells, the IGF-IR selectively promotes growth-unrelated processes, such as migration and invasion, but is not engaged in the transmission of growth and survival signals. Using ER-negative MDA-MB-231 breast cancer cells, we studied IGF-I-dependent pathways involved in migration and the defects in IGF mitogenic signal. For comparison, relevant IGF-I responses were analyzed in ER-positive MCF-7 cells.

Received 8/18/00; accepted 7/17/01.

The costs of publication of this article were defrayed in part by the payment of page charges. This article must therefore be hereby marked *advertisement* in accordance with 18 U.S.C. Section 1734 solely to indicate this fact.

[1] This work was supported by Department of Defense Breast Cancer Research Program Grants DAMD17-96-1-6250, DAMD17-97-1-7211, and DAMD-17-99-1-9407 and by the American-Italian Cancer Foundation.

[2] To whom requests for reprints should addressed, at Kimmel Cancer Center, Thomas Jefferson University, 233 South Tenth Street, BLSB 631, Philadelphia, PA 19107. Phone: (215) 503-4512; Fax: (215) 923-0249; E-mail: surmacz1@jeflin.tju.edu.

[3] The abbreviations used are: IGF-IR, insulin-like growth factor I receptor; IRS-1, insulin-receptor substrate 1; ER, estrogen receptor; GFP, green fluorescent protein; mAb, monoclonal antibody; WB, Western blot; CS, calf serum; IP, immunoprecipitation; pAb, polyclonal antibody; MAPK, mitogen-activated protein kinase; PI-3K, phosphatidylinositol 3-kinase; ERK, extracellular signal-regulated kinase; GSK, glycogen synthase kinase; MEK, MAPK kinase; PRF-SFM, phenol red-free serum-free medium.

MATERIALS AND METHODS

Plasmids. The pcDNA3-IGF-IR expression plasmid encoding the wild-type IGF-IR under the cytomegalovirus promoter was described before (13). The expression plasmids encoding constitutively active forms of Akt kinase, *i.e.*, myristylated Akt and Akt with an activating point mutation (Akt/E40K), were obtained from Drs. P. Tsichlis and T. Chan (Kimmel Cancer Center) and were described before (24). The Akt plasmids contain the HA-tag, allowing for easy identification of Akt-transfected cells. The pCMS-EGFP expression vector encoding GFP was purchased from Clontech.

Cell Lines. MDA-MB-231 cells were obtained from American Type Culture Collection. MDA-MB-231/IGF-IR clones were generated by stable transfection of MDA-MB-231 cells with the plasmid pcDNA3-IGF-IR using a standard calcium phosphate precipitate procedure (13). Transfectants resistant to 1 mg/ml G418 were screened for IGF-IR expression by fluorescence-assisted cell sorting analysis using an anti-IGF-IR mouse mAb α-IR3 (10 μg/ml; Calbiochem) and a fluorescein-conjugated goat antimouse IgG2 (1 μg/ml; Calbiochem). Cells stained with the secondary antibody alone were used as a control. Additionally, the parental MDA-MB-231 cells and MCF-7/IGF-IR clones 12 and 15 (13), all expressing known levels of the IGF-IR, were analyzed in parallel. IGF-IR expression in MDA-MB-213-derived clones was then confirmed by WB with specific antibodies (listed below). In growth and migration experiments, we used control MCF-7/pc2 and MDA-MB-231/5 M cell lines, which have been developed by transfection of MCF-7 and MDA-MB-231 cells with the pcDNA3 vector. MCF-7, MCF-7/pc2, and MCF-7/IGF-IR cells were described in detail previously (13).

Transient Transfection. Seventy % confluent cultures of MDA-MB-231 and MCF-7 cells were transiently cotransfected with an Akt expression plasmid and a plasmid pCMS encoding GFP (Akt:GFP ratio, 20:1) using Fugene 6 (Roche). Transfection was carried out for 6 h in phenol red-free DMEM containing 0.5 mg/ml BSA, 1 μM $FeSO_4$, and 2 mM L-glutamine (referred to as PRF-SFM; Ref. 13); the optimal DNA:Fugene 6 ratio was 1 μg:3 μl. Upon transfection, the cells were shifted to fresh PRF-SFM, and the expression of total and active Akt kinase at 0 (media shift), 2, and 4 days was assessed by WB with specific antibodies (see below). In parallel, the efficiency of transfection was evaluated by scoring GFP-positive cells. In all experiments, at least 40% of transfected cells expressed GFP, which indicated a high transfection efficiency. In addition, the expression of Akt plasmids was monitored by measuring the cellular levels of HA-tag and Akt proteins by WB.

Cell Culture. MDA-MB-231 and MCF-7 cells were grown in DMEM:F12 (1:1) containing 5% CS. MDA-MB-231- and MCF-7-derived clones overexpressing the IGF-IR or expressing vector alone were maintained in DMEM:F12 plus 5% CS plus 200 μg/ml G418. In the experiments requiring 17β-estradiol- and serum-free conditions, the cells were cultured in PRF-SFM (13).

Growth Curves. To analyze the growth in serum-containing medium, the cells were plated in six-well plates in DMEM:F12 (1:1) containing 5% CS at a concentration of 1.5–2.0 × 10^5 cells/plate; the number of cells was then assessed by direct counting at 1, 2, and 4 days after plating. To study IGF-I-dependent proliferation, the cells were plated in six-well plates in the growth medium as above. The following day (day 0), the cells at ~50% confluence were shifted to PRF-SFM containing 20 ng/ml IGF-I. Cell number was determined at days 1, 2, and 4.

Apoptosis Assay. The cells grown on coverslips in normal growth medium were shifted to PRF-SFM at 70% confluence and then cultured in the presence or absence of 20 ng/ml IGF-I for 0, 12, 24, 48, and 96 h. Apoptosis in the cultures was determined with the *In Situ* Cell Death Detection kit, Fluorescein (Roche), following the manufacturer's instructions. The cells containing DNA strand breaks were stained with fluorescein-dUTP and detected by fluorescence microscopy. Cells that detached during the experiment were spun on glass slides using cytospin and processed as above. Apoptotic index (the percentage of apoptotic cells/total cell number in a sample field) was determined for adherent and floating cell populations, and the indices were combined.

Immunoprecipitation and Western Blotting. Seventy % cultures were shifted to PRF-SFM for 24 h and then stimulated with 20 ng/ml IGF-I for 15 min, 1 h, 1 day, or 2 days. Proteins were obtained by lysing the cells in a buffer composed of 50 mM HEPES (pH 7.5), 150 mM 1% Triton X-100, 1.5 mM $MgCl_2$, 1 mM CaCl, 5 mM EGTA, 10% glycerin, 0.2 mM Na_3VO_4, [illegible] phenylmethylsulfonyl fluoride, and [illegible] aprotinin. The IGF-IR was immunoprecipitated from 500 μg of protein lysate with anti-IGF-IR mAb (Calbiochem) and subsequently detected by WB with anti-IGF-IR pAb (Santa Cruz Biotechnology). IRS-1 was precipitated from 500 μg of lysate with anti-IRS-1 pAb (UBI) and detected by WB using the same antibody. Tyrosine phosphorylation (PY) of immunoprecipitated IRS-1 or IGF-IR was assessed by WB with anti-phosphotyrosine mAb PY20 (Transduction Laboratories). Akt, ERK1/ERK2, and p38 MAPKs (active and total), and active GSK-3 were measured by WB in 50 μg of whole cell lysates with appropriate antibodies from New England Biolabs. The expression of HA-tag was probed by WB in 50 μg of protein lysate with anti-HA mAb (Babco). The intensity of bands representing relevant proteins was measured by laser densitometry scanning.

IRS-1-associated PI-3K Activity. PI-3K activity was determined *in vitro*, as described by us before (25). Briefly, 70% cultures were synchronized in PRF-SFM for 24 h and then stimulated with 20 ng of IGF-I for 15 min or 2 days. Untreated cells were used as controls. IRS-1 was precipitated from 500 μg of cell lysates; IRS-1 IPs were then incubated in the presence of inositol and [^{32}P]ATP for 30 min at room temperature. The products of the kinase reaction were analyzed by TLC using TLC plates (Eastman Kodak). Radioactive spots representing PI-3P were visualized by autoradiography, quantified by laser densitometry (ULTRO Scan XL, Pharmacia), and then excised from the plates and counted in a beta counter.

Motility Assay. Chemotaxis and chemokinesis were tested in modified Boyden chambers containing porous (8-mm), polycarbonate membranes. The membranes were not coated with extracellular matrix. Briefly, 2 × 10^4 cells (synchronized in PRF-SFM for 24 h) were suspended in 200 μl of PRF-SFM and plated into upper wells. Lower wells contained 500 μl of PRF-SFM. To study chemotaxis, IGF-I (20 ng/ml) was added to lower wells only; to assess chemokinesis, IGF-I was placed in either upper wells only, or in both wells. After 24 h, the cells in the upper wells were removed, whereas the cells that migrated to the lower wells were fixed and stained in Coomassie Blue solution (0.25 g of Coomassie blue:45 ml water:45 ml methanol:10 ml glacial acetic acid) for 5 min. After that, the chambers were washed three times with H_2O. The cells that migrated to the lower wells were counted under the microscope (10, 26).

Inhibitors of PI-3K and MAPK. LY294002 (Biomol Research Labs) was used to specifically inhibit PI-3K (27). UO126 (Calbiochem), a specific inhibitor of MEK1/2, was used to block ERK1 and ERK2 kinases (28), and SB203580 (Calbiochem) was used to down-regulate p38 MAPK (29). To determine optimal concentrations of the compounds, different doses (1–100 μM) of the inhibitors were tested in cells treated for 1, 8, 12, and 24 h in PRF-SFM. Additionally, the efficacy of all inhibitors in blocking the phosphorylation of relevant downstream targets (Akt, ERK1/ERK2, and p38 kinases) was determined by WB. In this experiment, the cells were stimulated with IGF-I (20 ng/ml) for 15 min. LY294002 and UO126 were supplemented simultaneously with IGF-I, whereas SB203580 was added 30 min before IGF-I treatment. Ultimately, for both growth and migration experiments, LY294002 was used at the concentration 50 μM, UO126 at 5 μM, and SB203580 at 10 μM. At these doses, the inhibitors did not affect cell proliferation and survival at 24 h, with the exemption of LY294002, which inhibited (by 20%) the proliferation of MCF-7/IGF-IR clone 12 in PRF-SFM. A shorter treatment (12 h) with LY294002 had no impact on the growth and survival of the cells (evaluated by cell proliferation and *In Situ* Cell Death Detection assays, as described above). Thus, the effects of LY294002 on migration were assessed at 12 h, whereas the actions of UO126 and SB203580 were assessed at 24 h of treatment.

RESULTS

MDA-MB-231/IGF-IR Cells. To study growth-related and growth-unrelated effects of IGF-I in ER-negative cells breast cancer cells, we used the MDA-MB-231 cell line. These cells express low levels of the IGF-IR and do not respond to IGF-I with growth (19, 22). Because it has been established that mitogenic response to IGF-I requires a threshold level of the IGF-IR (*e.g.*, in NIH 3T3-like fibroblasts, ~1.5 × 10^4 IGF-IRs; Refs. 30, 31), our first goal was to test whether increasing IGF-IR expression would induce IGF-I-dependent growth in MDA-MB-231 cells. To this end, several MDA-[illegible] clones overexpressing the IGF-IR (MDA-MB-231/IGF-IR

cells) were generated by stable transfection, and the receptor content was analyzed by binding assay, fluorescence-assisted cell sorting analysis (data not shown), and WB (Fig. 1). We determined that MDA-MB-231 clones 2, 21, and 31 express approximately 3×10^4, 1.5×10^4, and 2.5×10^5 IGF-IRs/cell, respectively, whereas the parental MDA-MB-231 cells express approximately 7×10^3 IGF-IRs/cell (19). For comparison, $\sim 6 \times 10^4$ IGF-IRs were found in ER-positive MCF-7 cells (Fig. 1; Ref. 13).

IGF-IR Overexpression Does Not Enhance the Growth of MDA-MB-231/IGF-IR Cells in Serum-containing Medium. The analysis of growth profiles of different MDA-MB-231/IGF-IR clones indicated that overexpression of the IGF-IR never improved basal proliferation in normal growth medium, and in the case of clone 31, which expressed the highest IGF-IR content ($\sim 2.5 \times 10^5$ IGF-IRs/cell), an evident growth retardation at days 2 and 4 ($P < 0.05$) was observed (Fig. 2*A*). In contrast, similar overexpression of the IGF-IR in ER-positive MCF-7 cells significantly augmented proliferation (Fig. 2*B*). The growth of control clones MDA-MB-231/5 M and MCF-7/pc2 was comparable with that of the corresponding parental cell lines (Fig. 2).

IGF-IR Overexpression Does Not Promote IGF-I-dependent Growth or Survival of MDA-MB-321 Cells. Subsequent studies established that increasing the levels of the IGF-IR from 7×10^3 up

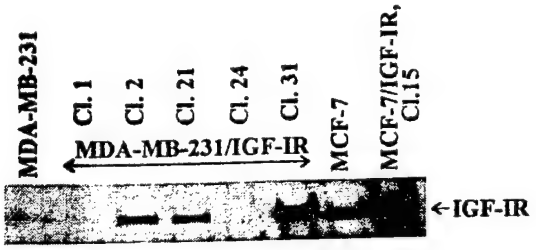

Fig. 1. MDA-MB-231/IGF-IR clones. MDA-MB-231/IGF-IR cells were generated by stable transfection with an IGF-IR expression vector, as described in "Materials and Methods." In several G418-resistant clones, the expression of the IGF-IR protein was tested in 50 μg of total protein lysate by WB with anti-β subunit IGF-IR pAb (Santa Cruz Biotechnology). For comparison, MCF-7 cells and MCF-7/IGF-IR clone 15 with known levels of IGF-IR (6×10^4 and 3×10^6, respectively; Ref. 13) are shown. Low levels of IGF-IR in MDA-MD-231 cells ($\sim 7 \times 10^3$ receptors/cell) are not well visible in this blot but were detectable in its phosphorylated form by IP and WB in 500 μg of protein lysates (see Fig. 4*A*). The estimated expression of the IGF-IR in clones 2, 21, and 31 is 1.5×10^4, 3×10^4, and 2.5×10^5 receptors/cell, respectively.

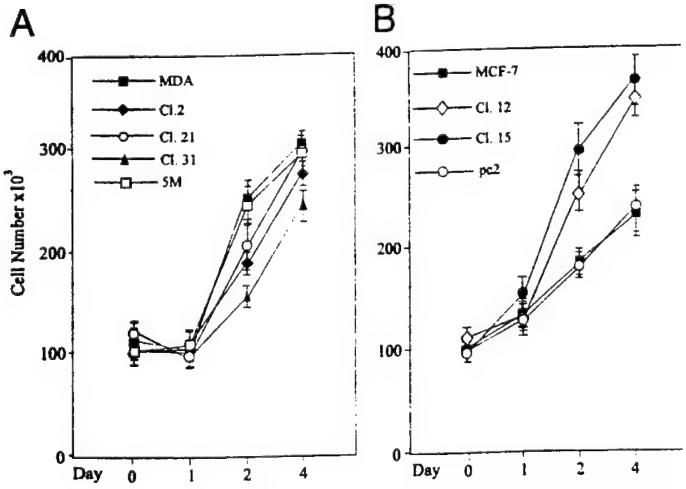

Fig. 2. Effect of IGF-IR overexpression on the growth of ER-negative and ER-positive cells in serum-containing medium. MDA-MB-231 cells, MDA-MB-231/IGF-IR clones 2, 21, and 31 (*A*), and their ER-positive counterparts, MCF-7 cells and MCF-7/IGF-IR clones ER 12 and 15 (*B*), were plated in DMEM:F12 plus 5% CS. The cells were counted at 50% confluence (day 0) and at subsequent days 1, 2, and 4. Control clones MDA-MB-231/5 M and MCF-7/pc2 expressing the pcDNA3 vector alone were used as controls (*A* and *B*). The results are averages from three experiments. *Bars*, SD.

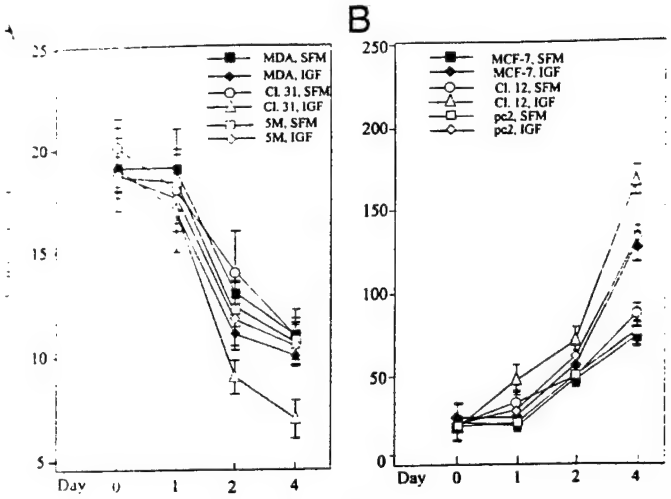

Fig. 3. IGF-I-dependent growth and survival of ER-negative and ER-positive breast cancer cells. ER-negative (*A*) and ER-positive (*B*) cells were synchronized in PRF-SFM and treated with IGF-I, as described in "Materials and Methods." The cells were counted on days 0, 1, 2, and 4 of treatment. The results are averages from at least three experiments. *Bars*, SD.

Table 1 *Effects of IGF-I on apoptosis in ER-negative and ER-positive cells*

Apoptosis was studied in MDA-MB-231 cells, MDA-MB-231/IGF-IR clone 31, MCF-7 cells, and MCF-7/IGF-IR clone 12. The cells were cultured for 48 h in PRF-SFM, and the apoptotic index (% apoptotic cells/total cell number in the field) was determined by terminal deoxynucleotidyl transferase-mediated nick end labeling, as described in "Materials and Methods." The results are averages from at least three experiments; SDs are given.

	Apoptosis (%)	
Cell line	SFM	SFM + IGF-I
MDA-MB-231	41.4 ± 3.0	46.0 ± 1.9
MDA-MB-231/IGF-IR	50.1 ± 4.1	53.3 ± 4.2
MCF-7	14.5 ± 0.2	4.2 ± 0.1
MCF-7/IGF-IR	10.1 ± 1.3	2.8 ± 0.1

2.5×10^5 was not sufficient to induce IGF-I-dependent growth response in MDA-MB-231 cells. In fact, similar to the parental and MDA-MB-231/5 M cells, all MDA-MB-231/IGF-IR clones were progressively dying in PRF-SFM with or without 20 ng/ml IGF-I (Fig. 3*A*). In all ER-negative cell lines, the rate of cell death was significantly increased at days 2 and 4 of the experiment. Notably, at these later time points, MDA-MB-231/IGF-IR clone 31 was dying faster in the presence of IGF-I than in PRF-SFM and more rapidly than the parental cells (Fig. 3*A* and data not shown). Conversely, in ER-positive cells, the stimulation of the IGF-IR always induced proliferation. In addition, at later time points, especially at day 4, the growth rate in IGF-I was significantly ($P < 0.05$) increased in MCF-7/IGF-IR cells relative to that in MCF-7 or MCF-7/pc2 cells (Fig. 3*B*).

The analysis of the antiapoptotic effects of IGF-I in the above cell lines cultured for 48 h under PRF-SFM indicated that IGF-I reduced apoptosis, by ~3-fold, in ER-positive cells, but it was totally ineffective in MDA-MB-231 and MDA-MB-231/IGF-IR cells (Table 1).

IGF-IR Signaling in MDA-MB-231 and MDA-MB-231/IGF-IR Cells. Next, we investigated molecular basis underlying the lack of IGF-I growth response in ER-negative cells. IGF-I signaling was studied in MDA-MB-231 cells, MDA-MB-231, clone 31, and in parallel, in ER-positive MCF-7 and MCF-7/IGF-IR cells. The experiments focused on IGF-IR tyrosine kinase activity and several post-receptor signaling pathways that are known to control the growth and survival of ER-positive breast cancer cells (and many other cell types), *i.e.*, the IRS-1/PI-3K, Akt, and ERK1/ERK2 pathways (1, 17, 32–34). We also analyzed other IGF-I effectors that have been

shown to contribute to nonmitogenic responses in ER-positive breast cancer cells, such as p38 kinase and SHC (10, 26, 35).

Because both acute and chronic effects of growth factors are important for biological response (36), we studied IGF-IR signaling at different times after stimulation: 15 min, 1 h, 2 days, and 4 days. In both ER-positive and ER-negative cell types, IGF-I signaling seen at 15 min was identical to that at 1 h, whereas IGF-I response at 2 days was similar to that at 4 days. Thus, Fig. 4 demonstrates the representative results obtained with cells stimulated for 15 min and 2 days. F4

In MDA-MB-231 and MDA-MB-231/IGF-IR cells, IGF-IR and its major substrate, IRS-1, were tyrosine phosphorylated at both time points in a manner roughly reflecting the receptor levels. The activation of both molecules was stronger just after stimulation and weaker at 2 days of the treatment (Fig. 4*A*). Analogous IGF-I effects were seen in MCF-7 cells and their IGF-IR-overexpressing derivatives (Fig. 4*B*). A basal level of IGF-IR and IRS-1 tyrosine phosphorylation was observed in cells expressing high receptor levels. This effect most likely can be attributed to the autocrine stimulation of the IGF-IR by IGF-I-like factors (12).

One of the major growth/survival pathways initiated at IRS-1 is the PI-3K pathway (32, 37). The repeated measurements of IRS-1-associated PI-3K activity *in vitro* demonstrated that at 15 min after IGF-I addition, PI-3K activity was similar in both cell types, but at 2 days, in MDA-MB-231 and MDA-MB-231/IGF-IR cells, IGF-I did not stimulate PI-3K through IRS-1, or induced it very weakly, whereas in MCF-7 and MCF-7/IGF-IR cells, a significant level of PI-3K activation was observed (Fig. 5). F5

The *in vitro* activity of PI-3K was reflected by the stimulation of its downstream effector, Akt kinase. At 15 min, Akt was up-regulated in response to IGF-I an all cell lines, but at 2 days, no effects of IGF-I were seen in MDA-MB-231 and MDA-MB-231/IGF-IR cells, whereas up-regulation of Akt was still evident in MCF-7 and MCF-7/IGF-IR cells (Fig. 4, *C* and *D*). Akt is known to phosphorylate (on Ser-9) and down-regulate GSK-3β (23, 32, 34). We found that in both cell types, the phosphorylation of GSK-3β reflected the dynamics of Akt activity, with no induction of phosphorylation observed at 2 days in ER-negative cells (Fig. 4*C*) and IGF-I-stimulated phosphorylation in MCF-7 and MCF-7/IGF-IR cells (by 40 and 120%, respectively; Fig. 4*D*).

Another IGF-IR growth/survival pathway involves ERK1 and ERK2 kinases (1, 36, 38). This pathway was strongly up-regulated at 15 min and weakly induced at 2 days in MCF-7 and MCF-7/IGF-IR cells. In MDA-MB-231 and MDA-MB-231/IGF-IR cells, the basal activation of ERK1/2 kinases was always high, and the addition of IGF-I only minimally (10–20%) induced the enzymes at 15 min, with no effects seen at 2 days (Fig. 4, *E* and *F*).

p38, a stress-induced MAPK and a known mediator of nongrowth responses in breast cancer cells (35), was strongly stimulated by IGF-I in ER-negative cells at 15 min (Fig. 4*E*). By contrast, in ER-positive cells, the enzyme was much stronger when induced at 2 days than at 15 min (Fig. 4*F*). The stimulation of SHC, a substrate of the IGF-IR involved in migration and growth in ER-positive cells (10, 26), was weak in all cell types, and no differences in the activation patterns were observed (data not shown).

Reactivation of Akt Kinase in MDA-MB-231 Cells. Previous results indicated that MDA-MB-231 and MDA-MB-231/IGF-IR cells are unable to sustain IGF-I-dependent activation of the PI-3K/Akt survival pathway when cultured in the absence of serum for 2–4 days. Consequently, we tested whether cell death under PRF-SFM conditions can be reversed by a forced overexpression of the Akt kinase. Two different expression plasmids encoding constitutively active forms of Akt, Myr-Akt, and Akt/E40K (24) were transiently transfected into MDA-MB-231 cells. The efficiency of transfection was at least 40% (by scoring GFP-positive cells); correspondingly, the transfected cells expressed elevated (by ~40%) levels of the Akt protein and exhibited enhanced Akt phosphorylation (Fig. 6*A*). The improved biological activity of Akt in the transfected cells was indicated by down-regulation of the prolonged ERK1/2 stimulation (39, 40), which was noticeable at day 2 (data not shown) and most pronounced at day 4 (~50 and 40% for Myr-Akt and Akt/E40K, respectively; Fig. 6*B*) The expression of constitutively active Akt mutants was reflected by a tendency of MDA-MB-231 cells to survive better at 2 days after transfection (at the time of the greatest Akt activity), but the differ- F6

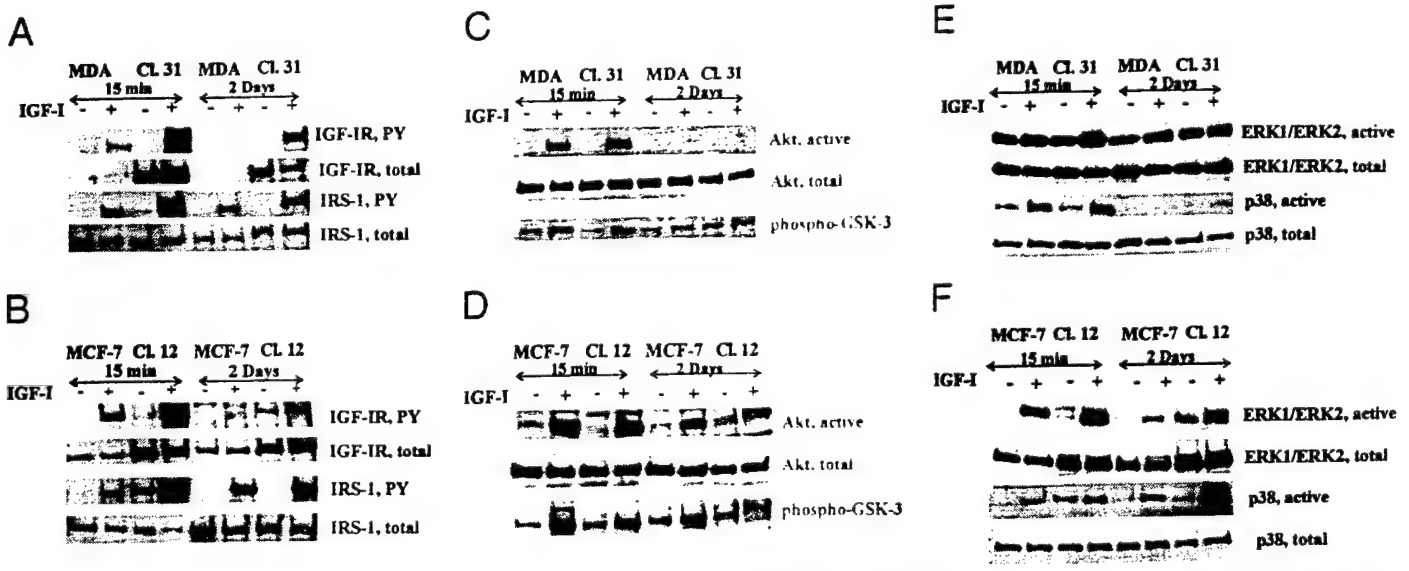

Fig. 4. IGF-I signaling in ER-negative and ER-positive breast cancer cells. The activation of IGF-IR/IRS-1 signaling (*A* and *B*), Akt/GSK-3 signaling (*C* and *D*), and ERK1/ERK2 and p38 kinase signaling (*E* and *F*) was tested in MDA-MB-231 cells, MDA-MB-231/IGF-IR clone 31, MCF-7 cells, and MCF-7/IGF-IR clone 12. The cells were synchronized in PRF-SFM and treated with IGF-I for 15 min or 2 days. The cellular levels of the IGF-IR and IRS-1 were detected by IP and WB in 500 μg of total protein lysate using specific antibodies (see "Materials and Methods"). IGF-IR and IRS-1 tyrosine phosphorylation (PY) was assessed upon stripping and reprobing the same filters with the anti-PY20 antibody. The levels and activity of Akt, GSK-3, ERK1/ERK2, and p38 kinases were probed by WB in 50 μg of total cellular lysates using specific antibodies. The antibodies used are listed in "Materials and Methods." Representative results of at least three repeats are shown. Note decreased IRS-1 expression in 2 *min IGF-I* treatment in ER-positive cells, as described before (47).

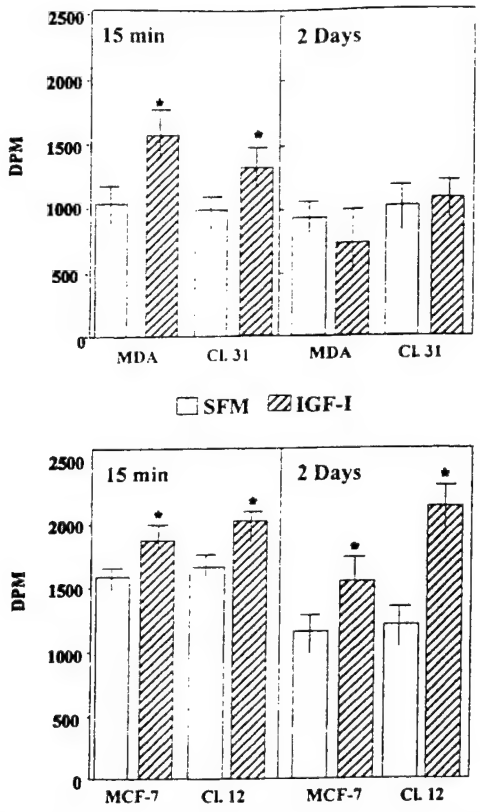

Fig. 5. IGF-I-induced PI-3K activity in ER-negative and ER-positive cells. MDA-MB-231 cells, MDA-MB-231/IGF-IR clone 31, MCF-7 cells, and MCF-7/IGF-IR clone 12 were synchronized in PRF-SFM and treated with IGF-I for 15 min or 2 days. IRS-1-bound PI-3K activity was measured *in vitro* in IRS-1 IPs as described in "Materials and Methods." The experiments were repeated three times for ER-positive cells and five times for ER-negative cells. *Bars*, SD. *, statistically significant differences between untreated and IGF-I-treated cells.

ences did not reach statistical significance ($P > 0.05$; Fig. 6*C* and data not shown).

Inhibition of IGF-IR Signaling Pathways. To complement the above studies, we examined the importance of the PI-3K, ERK1/ERK2, and p38 kinase pathways in IGF-I-dependent growth and survival of ER-positive and ER-negative breast cancer cells using specific inhibitors (27–29). The efficacy of PI-3K and ERK1/ERK2 inhibitors was first tested by establishing their effects on the activity of target proteins (Fig. 7). Table 2 demonstrates the impact of the compounds on cell growth/survival at 2 days of treatment. The inhibition of PI-3K with LY294002 reduced the growth of MCF-7 and MCF-7/IGF-IR cells, but it did not influence or had only minimal effects on MDA-MB-231 and MDA-MB-231/IGF-IR cells. Furthermore, the action of LY294002 was counteracted by IGF-I in ER-positive, but not in ER-negative, cells. The inhibition of MEK1/2 and ERK1/ERK2 with UO126 reduced the growth and/or survival in both cell types, but only in MCF-7 and MCF-7/IGF-IR cells was IGF-I able to oppose this effect. Down-regulation of p38 kinase with SB203580 reduced the survival of MDA-MB-231 and MDA-MB-231/IGF-IR cells and to a lesser extent the growth and survival of MCF-7 and MCF-7/IGF-IR cells. IGF-I did not reverse the antimitogenic action of the p38 kinase inhibitor in either of the cell lines studied (Table 2). Cumulatively, these results suggested that in ER-positive cells, IGF-I transmits mitogenic signals through PI-3K and ERK1/ERK2 pathways. By contrast, IGF-I does not induce growth or survival signal through these pathways in ER-negative cells.

IGF-I Stimulates Migration of MDA-MB-231 Cells. We investigated the nonmitogenic effects of IGF-I in ER-negative and ER-positive breast cancer cells. Unlike with the growth and survival responses, we found that the IGF-IR transmitted nonmitogenic signals in MDA-MB-231 and MDA-MB-231/IGF-IR cells. Specifically, in the chemotaxis experiments, IGF-I placed in lower wells stimulated migration of ER-negative cells in a manner reflecting IGF-IR content. Similarly, the same IGF-I doses induced migration in ER-positive cells (Table 3). The addition of IGF-I to the upper well or both upper and lower wells always suppressed chemotaxis of all cell lines (Table 3).

IGF-I Pathways Regulating Migration of MDA-MB-231 Cells. Using the inhibitors of PI-3K, ERK1/ERK2, and p38 kinases, we determined which pathways of the IGF-IR are involved in migration of ER-negative and ER-positive cells. The treatment was carried out for 24 h (UO126 and SB203580) or 12 h (LY294002) and did not affect cell growth and/or survival with or without IGF-I (see "Materials and Methods"). As demonstrated in Table 4, down-regulation of PI-3K with LY294002 inhibited basal migration of both cell types, with a more pronounced effect in ER-negative cells. Similarly, blockade of p38 kinase inhibited motility of all cell lines studied. The inhibition of MEK1/2 and ERK1/2 with UO126 never suppressed the

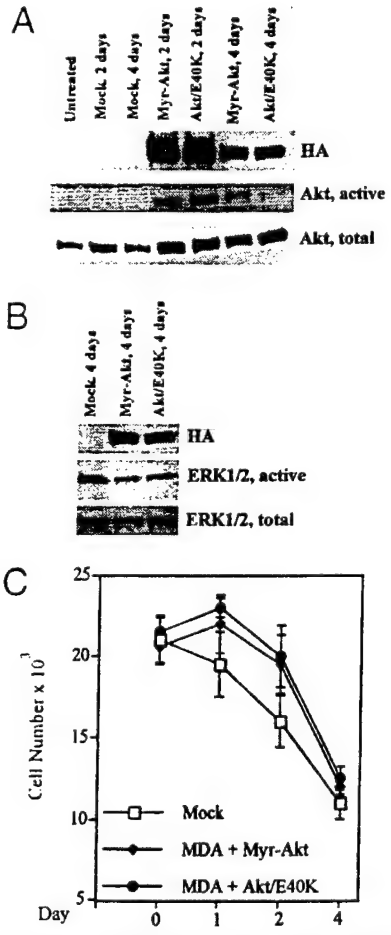

Fig. 6. Effect of increased Akt activity on the survival of MDA-MB-231 cells. MDA-MB-231 cells were transiently transfected with expression plasmids encoding two different constitutively active Akt kinase mutants (Myr-Akt and Akt/E40K; Ref. 24). The Akt vectors contained HA-tag for easy detection. The cells treated with the transfection mixture lacking plasmid DNA (*Mock*) served as control. The expression of the plasmids, as well as the activity and the levels of Akt kinase in the transfected cells, was monitored at 2 and 4 days after transfection. Fifty μg of total protein lysates were sequentially probed by WB with anti-HA, anti-active Akt and then anti-total Akt-specific antibodies (described in "Materials and Methods"). Representative results of four repeats are shown (*A*). To assess biological activity of Akt, the levels of total and active ERK1/2 in cells transfected with the Myr-Akt expression vector were probed in 50 μg of total cell lysate using specific antibodies; the inhibition of ERK1/2 at 4 days after transfection is shown (*B*). *C*, in parallel, the number of cells was determined at days 0 (posttransfection medium change), 1, 2, and 4 after transfection. The results are averages from four experiments. *Bars*, SD

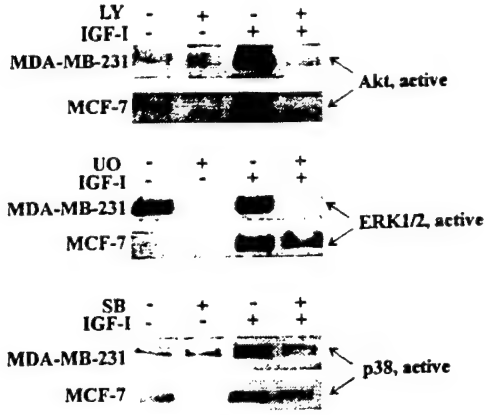

Fig. 7. PI-3K and MAPK inhibitors. Synchronized cultures of MDA-MB-231 and MCF-7 cells were treated with LY294002, UO126, or SB203580 in the presence or absence of IGF-I, as described in "Materials and Methods." The activities of Akt, ERK1/ERK2, and p38 kinases were determined by WB in 50 μg of protein lysates using specific antibodies. Representative results are shown.

migration of ER-positive and ER-negative cells; in fact, the compound stimulated cell motility. The addition of IGF-I as a chemoattractant significantly counteracted the effects of all three inhibitors; however, no clear association between the cellular levels of the IGF-IR and this competing action of IGF-I was noted (Table 4). These results suggested that IGF-I-dependent motility in both types of cells requires the PI-3K and p38 pathways but does not rely on the activity of ERK1/ERK2.

DISCUSSION

The experimental and clinical evidence supports the notion that hyperactivation of the IGF-IR may be critical in early steps of breast cancer development, promoting cell growth, survival, and resistance to therapeutic treatments. However, the function of the IGF-IR in the later stages of the disease, including metastasis, is still obscure (1). For instance, whereas the IGF-IR has been found overexpressed in primary breast tumors, its levels, similar to ER levels, appear to undergo reduction during the course of the disease (1, 18). According to Pezzino *et al.* (41), who studied the IGF-IR status in two patient subgroups representing either a low risk (ER- and progesterone receptor-positive, low mitotic index, diploid) or a high risk (ER- and progesterone receptor-negative, high mitotic index, aneuploid) population, there is a highly significant correlation between IGF-IR expression and better prognosis. Similar conclusions were reached by Peyrat and Bonneterre (42) and recently by Schnarr *et al.* (18). Therefore, it has been proposed that similar to the ER, the IGF-IR marks more differentiated tumors with better clinical outcome. However, it has also been argued that the IGF-IR may play a role in early steps of tumor spread because node-positive/IGF-IR-positive tumors appeared to have a worse prognosis than node-negative/IGF-IR-positive tumors (1, 42). In addition, quite rare cases of ER-negative but IGF-IR-positive tumors are associated with shorter disease-free survival (43).

In breast cancer cell lines, a hormone-dependent and less aggressive phenotype correlates with a good IGF-IR expression (1, 19, 42). By contrast, different ER-negative, breast cancer cell lines express low levels of the IGF-IR and generally do not respond to IGF-I with growth (1, 18–22). However, many ER-negative cell lines appear to depend on the IGF-IR for tumorigenesis and metastasis. For instance, blockade of the IGF-IR in MDA-MB-231 cells by anti-IGF-IR antibody reduced migration *in vitro* and tumorigenesis *in vivo*, and expression of a soluble IGF-IR in MDA-MB-435 cells impaired growth, tumorigenesis, and metastasis in animal models (1, 14, 16, 23). These observations suggest that some growth-unrelated pathways of the IGF-IR may be operative in the context of ER-negative cells.

Here we studied whether this particular IGF-I dependence of ER-negative breast cancer cells relates to the nonmitogenic function of the IGF-IR, such as cell migration. Our experiments indicated that the IGF-IR is an effective mediator of cell motility. Furthermore, IGF-I-induced migration was proportional to IGF-IR content. We demonstrated, for the first time, that in MDA-MB-231 ER-negative cells, IGF-IR signaling pathways responsible for cell movement include PI-3K and p38 kinases. Indeed, an acute IGF-I stimulation of MDA-MB-231 and MDA-MB-231/IGF-IR cells appears to induce both PI-3K and p38 kinases, suggesting that this short-time activation may be involved in migration. Both of these pathways have been shown previously to regulate cell motility in breast cancer cells and other cell types (35, 44). Interestingly, the migration of both ER-negative and ER-positive cells was enhanced by a specific MEK1/MEK2 inhibitor UO126. We observed this effect over a broad range of UO126 doses (1–10 μM) and in several MDA-MB-231- and MCF-7-derived clones; the same doses always suppressed cell proliferation in serum-containing medium and PRF-SFM (data not shown and Table 2). These

Table 3 *IGF-I-induced migration in ER-negative and ER-positive breast cancer cells*

The IGF-I-induced migration of MDA-MB-231 and MCF-7 cells, their IGF-IR-overexpressing derivatives, as well as control clones MDA-MB-231/5M and MCF-7/pc2, was determined after 24 hr, as described in "Materials and Methods." At this time point, IGF-I did not produce statistically significant differences in the growth and survival of the cells studied (Fig. 3). Migration (%) represents the difference (in %) between basal migration in PRF-SFM and migration in the presence of IGF-I. The chemotaxis results are averages (±SE) from at least nine experiments. The chemokinesis results are averages (±SE) from three experiments.

	Migration (%)[a]		
Cell line	Lower well	Upper well	Both wells
MDA-MB-231	+24 ± 3.9	+2 ± 0.1	+7 ± 0.4
MDA-MB-231/IGF-IR	+79 ± 4.1	+10 ± 0.1	+12 ± 0.5
MDA-MB-231/5M	+20 ± 2.0	+1 ± 0.0	+5 ± 0.1
MCF-7	+23 ± 4.7	−1 ± 0.0	−2 ± 0.0
MCF-7/IGF-IR	+47 ± 5.6	−10 ± 0.5	−8 ± 0.2
MCF-7/pc2	+17 ± 3.1	0 ± 0.0	−1 ± 0.0

[a] IGF-I.

Table 2 *Effects of PI-3K and MAPK inhibitors on growth and survival of ER-negative and ER-positive breast cancer cells*

MDA-MB-231 cells, MDA-MB-231/IGF-IR clone 31, MCF-7 cells, and MCF-7/IGF-IR clone 12 were cultured in PRF-SFM with or without IGF-I in the presence or absence of the inhibitors for 48 h, as described in "Materials and Methods." The difference (in percentages) between the number of live cells under treatment and the number of cells cultured under control conditions (without inhibitors) was defined as inhibition (%). The results are averages from three experiments; SDs are given.

	Inhibition (%)					
	LY294002 (PI-3K)		UO126 (MEK)		SB203580 (p38)	
Cell line	SFM	+IGF	SFM	+IGF	SFM	+IGF
MDA-MB-231	9.4 ± 1.0	7.8 ± 0.8	35.0 ± 2.6	39.0 ± 2.7	47.8 ± 2.2	42.5 ± 4.4
MDA-MB-231/IGF-IR	11.1 ± 1.2	12.3 ± 0.9	18.3 ± 0.9	22.9 ± 1.3	29.5 ± 2.0	35.6 ± 3.6
MCF-7	68.8 ± 3.3	35.0 ± 1.2	42.6 ± 3.8	26.3 ± 2.5	11.7 ± 1.2	10.0 ± 0.4
MCF-7/IGF-IR	73.2 ± 6.7	34.6 ± 2.7	49.4 ± 3.9	20.2 ± 1.5	24.7 ± 0.2	25.9 ± 0.9

Table 4 *Effects of PI-3K and MAPK inhibitors on migration of ER-negative and ER-positive breast cancer cells*

The migration of MDA-MB-231 cells, MDA-MB-231/IGF-IR clone 31, MCF-7 cells, and MCF-7/IGF-IR clone 12 was tested in modified Boyden chambers as described in "Materials and Methods." The inhibitors were added to the upper wells at the time of cell plating, and their effect on basal (SFM) or IGF-I-induced (+IGF) migration was assessed after 24 h (for UO126 and SB203580) or 12 h (for LY94002). At these time points, the compounds did not affect cell growth and survival. The values represent the percentage of change relative to the migration at basal conditions in PRF-SFM (SFM) without inhibitors or chemoattractants. The experiments were repeated at least three times; the average results (±SD) are given.

	Change (%)					
	LY294002 (PI-3K)		UO126 (MEK)		SB203580 (p38)	
Cell line	SFM	+IGF	SFM	+IGF	SFM	+IGF
MDA-MB-231	−45.1 ± 1.1	−18.9 ± 0.9	+53.4 ± 3.5	+36.4 ± 2.2	−30.2 ± 2.9	−8.5 ± 0.7
MDA-MB-231/IGF-IR	−38.3 ± 3.5	−12.2 ± 0.4	+29.0 ± 2.0	+12.6 ± 0.7	−40.1 ± 0.4	−2.5 ± 0.0
MCF-7	−24.7 ± 1.2	−9.6 ± 0.9	+94.9 ± 3.9	+56.4 ± 1.7	−18.9 ± 1.1	−5.6 ± 0.2
MCF-7/IGF-IR	−20.4 ± 1.0	−8.0 ± 0.7	+65.6 ± 5.4	+23.8 ± 1.9	−24.8 ± 0.8	−1.7 ± 0.1

peculiar effects suggest that MEK1/2 may represent a regulatory point balancing mitogenic and nonmitogenic cell responses.

In contrast with the positive effects of IGF-I on cell motility in ER-negative and ER-positive breast cancer cells, this growth factor never stimulated the proliferation of MDA-MB-231 cells, whereas it induced the growth of MCF-7 cells and MCF-7-derived clones overexpressing the IGF-IR. It is has been established by Rubini *et al.* (30) and Reiss *et al.* (31) that mitogenic response to IGF-I requires a threshold level of IGF-IR expression (in fibroblasts, $\sim 1.5 \times 10^4$). Here, we demonstrated that increasing the levels of the IGF-IR from $\sim 7 \times 10^3$ up to $\sim 2.5 \times 10^5$ and subsequent up-regulation of IGF-IR tyrosine phosphorylation was not sufficient to induce IGF-I-dependent growth of MDA-MB-213 cells. Similar results were obtained by Jackson and Yee (21), who showed that overexpression of IRS-1 in ER-negative MDA-MB-435A and MDA-MB-468 breast cancer cells did not stimulate IGF-I-dependent mitogenicity. These authors suggested that the lack of IGF-I response, even in IRS-1-overexpressing ER-negative cells, was related to insufficient stimulation of ERK1/ERK2 and PI-3K pathways (21). Defective insulin response in ER-negative cell lines has also been described by Costantino *et al.* (45) and linked with an increased tyrosine phosphatase activity.

Our experiments suggested that the lack of IGF-I mitogenicity in MDA-MB-231 and MDA-MB-231/IGF-IR cells was not related to the impaired IGF-IR or IRS-1 tyrosine phosphorylation. The cells were also able to respond to an acute IGF-I stimulation with a marked activation of the PI-3K/Akt and ERK-1/ERK2 pathways. We hypothesize that this transient stimulation could be sufficient to induce some IGF-I response, such as cell motility. Mitogenic response, on the other hand, may rely on a more sustained activation of critical IGF-IR signals, as demonstrated before with mouse embryo fibroblasts (36). Indeed, the most significant difference in IGF-I signal between ER-negative and ER-positive cells rested in the impaired long-term stimulation of the PI-3K/Akt pathway; MDA-MB-231 and MDA-MB-231/IGF-IR cells were unable to sustain this IGF-I-induced signal for 1 or 2 days, whereas in MCF-7 and MCF-7/IGF-IR cells, the PI-3K/Akt pathway was still active at this time. The subsequent experiments with MDA-MB-231 cells transfected with constitutively active Akt mutants demonstrated that the increased biological activity of Akt was not sufficient to completely reverse cell death in PRF-SFM (Fig. 6*C* and data not shown). This suggested that although a sustained Akt activity could be important in the survival of breast cancer cells, other pathways, or a proper equilibrium between Akt and other pathways (such as ERK1/2), are also critical. The latter possibility could be supported by our finding that hyperactivation of Akt down-regulates the ERK1/2 pathway. Normally, this pathway appears to play a role in the survival of ER-negative cells (Table 2).

In summary, our data suggest that IGF-IR signaling and function may be different in hormone-dependent and -independent breast cancer cells. In ER-positive MCF-7 cells, IGF-IR transmits various signals, such as growth, survival, migration, and adhesion. In ER-negative MDA-MB-231 cells, the growth-related functions of the IGF-IR become attenuated, but the receptor is still able to control nonmitogenic processes, such as migration. It is likely that this kind of evolution is also involved with the response to other growth factors. Epidermal growth factor, for instance, is an effective mitogen for ER-positive breast cancer cells but does not stimulate the proliferation or survival in MDA-MB-231 cells, despite high EGF-R expression (46). However, as demonstrated recently by Price *et al.* (46), EGF is a potent chemoattractant for MDA-MB-231 cells. EGF-induced migration in MDA-MB-231 cells requires PI-3K and phospholipase Cγ and is not inhibited by antagonists of ERK1/ERK2.

In conclusion, mitogenic and nonmitogenic pathways induced by growth factors in breast cancer cells may be dissociated, and attenuation of one is not necessarily linked with the cessation of the other. Delineating the nonmitogenic responses will be critical for the development of drugs specifically targeting metastatic cells.

REFERENCES

1. Surmacz, E. Function of the IGF-IR in breast cancer. J. Mammary Gland Biol. Neopl., *5:* 95–105, 2000.
2. Baserga, R. The IGF-I receptor in cancer research. Exp. Cell Res., *253:* 1–6, 1999.
3. Kleinberg, D. L., Feldman, M., and Ruan, W. J. IGF-I: an essential factor in terminal end bud formation and ductal morphogenesis. Mammary Gland Biol. Neopl., *5:* 7–17, 2000.
4. Turner, B. C., Haffty, B. G., Narayanann, L., Yuan, J., Havre, P. A., Gumbs, A., Kaplan, L., Burgaud, J-L., Carter, D., Baserga, R., and Glazer, P. M. IGF-I receptor and cyclin D1 expression influence cellular radiosensitivity and local breast cancer recurrence after lumpectomy and radiation. Cancer Res., *57:* 3079–3083, 1997.
5. Resnik, J. L., Reichart, D. B., Huey, K., Webster, N. J. G., and Seely, B. L. Elevated insulin-like growth factor I receptor autophosphorylation and kinase activity in human breast cancer. Cancer Res., *58:* 1159–1164, 1998.
6. Rocha, R. L., Hilsenbeck, S. G., Jackson, J. G., Van Der Berg, C. L., Weng, C-W., Lee, A. V., and Yee, D. Insulin-like growth factor binding protein 3 and insulin receptor substrate 1 in breast cancer: correlation with clinical parameters and disease-free survival. Clin. Cancer Res., *3:* 103–109, 1997.
7. Lee, A. V., Jackson, J. G., Gooch, J. L., Hilsenbeck, S. G., Coronado-Heinsohn, E., Osborne, C. K., and Yee, D. Enhancement of insulin-like growth factor signaling in human breast cancer: estrogen regulation of insulin receptor substrate-1 expression *in vitro* and *in vivo*. Mol. Endocrinol., *10:* 787–796, 1999.
8. Hankinson, S. E., Willet, W. C., Colditz, G. A., Hunter, D. J., Michaud, D. S., Deroo, B., Rosner, B., Speitzer, F. E., and Pollak, M. Circulating concentrations of insulin-like growth factor and risk of breast cancer. Lancet, *35:* 1393–1396, 1998.
9. Dunn, S. E., Hardman, R. A., Kari, F. W., and Barrett, J. C. Insulin-like growth factor 1 (IGF-1) alters drug sensitivity of HBL100 human breast cancer cells by inhibition of apoptosis induced by diverse anticancer drugs. Cancer Res., *57:* 2687–2693, 1997.
10. Nolan, M., Jankowska, L., Prisco, M., Xu, S., Guvakova, M., and Surmacz, E. Differential roles of IRS-1 and SHC signaling pathways in breast cancer cells. Int. J. Cancer, *72:* 828–834, 1997.
11. Gooch, J. L., Van Den Berg, C. L., and Yee, D. Insulin-like growth factor (IGF)-I rescues breast cancer cells from chemotherapy-induced cell death—proliferative and anti-apoptotic effects. Breast Cancer Res. Treat., *56:* 1–10, 1999.
12. Surmacz, E., and Burgaud, J-L. Overexpression of IRS-1 in the human breast cancer cell line MCF-7 induces loss of estrogen requirements for growth and transformation. Clin. Cancer Res., *1:* 1429–1436, 1995.
13. Guvakova, M. A., and Surmacz, E. Overexpressed IGF-I receptors reduce estrogen growth requirements, enhance survival and promote cell-cell adhesion in human breast cancer cells. Exp. Cell Res., *231:* 149–162, 1997.

14. Dunn, S. E., Ehrlich, M., Sharp, N. J. H., Reiss, K., Solomon, G., Hawkins, R., Baserga, R., and Barrett, J. C. A dominant negative mutant of the insulin-like growth factor I receptor inhibits the adhesion, invasion and metastasis of breast cancer. Cancer Res., *58*: 3353–3361, 1998.
15. Neuenschwander, S., Roberts, C. T., Jr., and LeRoith, D. Growth inhibition of MCF-7 breast cancer cells by stable expression of an insulin-like growth factor I receptor antisense ribonucleic acid. Endocrinology, *136*: 4298–4303, 1995.
16. Arteaga, C. L., Kitten, L. J., Coronado, E. B., Jacobs, S., Kull, F. C., Jr., Allred, D. C., and Osborne, C. K. Blockade of the type I somatomedin receptor inhibits growth of human breast cancer cells in athymic mice. J. Clin. Invest., *84*: 1418–1423, 1989.
17. Jackson, J. G., White, M. F., and Yee, D. Insulin receptor substrate-1 is the predominant signaling molecule activated by insulin-like growth factor I, insulin, and interleukin-4 in estrogen receptor-positive human breast cancer cells. J. Biol. Chem., *273*: 9994–10003, 1998.
18. Schnarr, B., Strunz, K., Ohsam, J., Benner, A., Wacker, J., and Mayer, D. Down-regulation of insulin-like growth factor-I receptor and insulin receptor substrate-1 expression in advanced human breast cancer. Int. J. Cancer, *89*: 506–513, 2000.
19. Peyrat, J. P., Bonneterre, J., Dusanter-Fourt, I., Leroy-Martin, B., Dijane, J., and Demaille, A. Characterization of insulin-like growth factor I receptors (IGF-IR) in human breast cancer cell lines. Bull. Cancer, *76*: 311–309, 1989.
20. Sepp-Lorenzino, L., Rosen, N., and Lebwohl, D. Insulin and insulin-like growth factor signaling are defective in MDA-MB-468 human breast cancer cell line. Cell Growth Differ., *5*: 1077–1083, 1994.
21. Jackson, J., and Yee, D. IRS-1 expression and activation are not sufficient to activate downstream pathways and enable IGF-I growth response in estrogen receptor negative breast cancer cells. Growth Horm. IGF Res., *9*: 280–289, 1999.
22. Godden, J., Leake, R., and Kerr, D. J. The response of breast cancer cells to steroid and peptide growth factors. Anticancer Res., *12*: 1683–1688, 1992.
23. Doerr, M., and Jones, J. The roles of integrins and extracellular matrix proteins in the IGF-IR-stimulated chemotaxis of human breast cancer cells. J. Biol. Chem., *271*: 2443–2447, 1996.
24. Chan, T. O., Rittenhouse, S. E., and Tsichlis, P. N. AKT/PKB and other D3 phosphoinositide-regulated kinases: kinase activation by phosphoinositide-dependent phosphorylation. Annu. Rev. Biochem., *68*: 965–1014, 1999.
25. Guvakova, M. A., and Surmacz, E. Tamoxifen interferes with the insulin-like growth factor I receptor (IGF-IR) signaling pathway in breast cancer cells. Cancer Res., *57*: 2606–2610, 1997.
26. Mauro, L., Sisci, D., Bartucci, M., Salerno, M., Kim, J., Tam, T., Guvakova, M., Ando, S., and Surmacz, E. SHC-$\alpha_5\beta_1$ integrin interactions regulate breast cancer cell adhesion and motility. Exp. Cell Res., *252*: 439–448, 1999.
27. Vlahos, C. J., Matter, W. F., Hui, K. Y., and Brown, R. F. A specific inhibitor of phosphatidylinositol 3-kinase, 2-(4-morpholinyl)-8-phenyl-4*H*-1-benzopyran-4-one (LY294002). J. Biol. Chem., *269*: 5241–5248, 1994.
28. Favata, M., Horiuchi, K. Y., Manos, E., Daulerio, A. J., Stradley, D. A., Feeser, W. S., van Dyk, D. E., Pitts, W. J., Earl, R. A., Hobbs, F., Copeland, R. A., and Magolda, R. L. Identification of a novel inhibitor of mitogen-activated protein kinase kinase. J. Biol. Chem., *273*: 18623–18632, 1998.
29. Lee, J. C., Kassis, S., Kumar, S., Badger, A., and Adams, J. p38 mitogen-activated protein kinase inhibitors—mechanisms and therapeutic potentials. Pharmacol. Ther., *82*: 389–397, 1999.
30. Rubini, M., Hongo, A., D'Ambrosio, C., and Baserga, R. The IGF-IR in mitogenesis and transformation of mouse embryo fibroblasts: role of receptor number. Exp. Cell Res., *230*: 284–292, 1997.
31. Reiss, K., Valentinis, B., Tu, X., Xu, S-Q., and Baserga, R. Molecular markers of IGF I-mediated mitogenesis. Exp. Cell Res., *242*: 361–372, 1998.
32. Shepherd, P. R., Withers, D., and Siddle, K. Phosphoinositide3-kinase: the key switch mechanism in insulin signalling. Biochem. J., *333*: 471–490, 1998.
33. Dufourny, B., Alblas, J., van Teeffelen, H. A., van Schaik, F. M., van der Burg, B., Steenbergh, P. H., and Sussenbach, J. S. Mitogenic signaling of insulin-like growth factor I in MCF-7 human breast cancer cells requires phosphatidylinositol 3-kinase and is independent of mitogen-activated protein kinase. J. Biol. Chem., *272*: 31163–31171, 1997.
34. Vanhaesebroeck, B., and Alessi, D. R. The PI3K-PDK1 connection: more than just a road to PKB. Biochem. J., *15*: 561–576, 2000.
35. Huang, S., New, L., Pan, Z., Han, J., and Nemerow, G. L. Urokinase plasminogen activator/urokinase-specific surface receptor expression and matrix invasion by breast cancer cells requires constitutive p38α mitogen-activated protein kinase activity. J. Biol. Chem., *275*: 12266–12272, 2000.
36. Swantek, J. L., and Baserga, R. Prolonged activation of ERK2 by epidermal growth factor and other growth factors requires a functional insulin-like growth factor I receptor. Endocrinology, *140*: 3163–3169, 1999.
37. White, M. F. The IRS-signalling system: a network of docking proteins that mediate insulin action. Mol. Cell. Biochem., *182*: 3–11, 1998.
38. Peruzzi, F., Prisco, M., Dews, M., Salomoni, P., Grassilli, E., Romano, G., Calabretta, B., and Baserga, R. Multiple signaling pathways of the insulin-like growth factor 1 receptor in protection from apoptosis. Mol. Cell. Biol., *19*: 7203–7215, 1999.
39. Zimmermann, S., and Moelling, K. Phosphorylation and regulation of Raf by Akt (protein kinase B). Science (Wash. DC), *286*: 1741–1744, 1999.
40. Rommel, C., Clarke, B. A., Zimmermann, S., Nunez, L., Rossman, R., Reid, K., Moelling, K., Yancopoulos, G. D., and Glass, D. J. Differentiation stage-specific inhibition of the Raf-MEK-ERK pathway by Akt. Science (Wash. DC), *286*: 1738–1740, 1999.
41. Pezzino, V., Papa, V., Milazzo, G., Gliozzo, B., Russo, P., and Scalia, P. L. Insulin-like growth factor-I (IGF-I) receptors in breast cancer. Ann. NY Acad. Sci., *784*: 189–201, 1996.
42. Peyrat, J. P., and Bonneterre, J. Type 1 IGF receptor in human breast diseases. Breast Cancer Res. Treat., *22*: 59–67, 1992.
43. Railo, M. J., Smitten, K., and Pekonen, F. The prognostic value of insulin-like growth factor I in breast cancer. Results of a follow-up study on 126 patients. Eur. J. Cancer, *30A*: 307–311, 1994.
44. Guvakova, M., and Surmacz, E. The activated insulin-like growth factor I receptor induces depolarization in breast cancer cells characterized by actin filament disassembly and tyrosine dephosphorylation of FAK, Cas, and paxillin. Exp. Cell Res., *251*: 244–255, 1999.
45. Costantino, A., Milazzo, G., Giorgino, F., Russo, P., Goldfine, I. D., Vigneri, R., and Belfiore, A. Insulin-resistant MDA-MB231 human breast cancer cells contain a tyrosine kinase inhibiting activity. Mol. Endocrinol., *7*: 1667–1679, 1993.
46. Price, J. T., Tiganis, T., Agarwal, A., Djakiew, D., and Thompson, E. W. Epidermal growth factor promotes MDA-MB-231 breast cancer cell migration through a phosphatidylinositol 3'-kinase and phospholipase C-dependent mechanism. Cancer Res., *59*: 5475–5478, 1999.
47. Lee, A. V., Gooch, J. L., Oesterreich, S., Guler, R. L., and Yee, D. Insulin-like growth factor I-induced degradation of insulin receptor substrate 1 is mediated by the 26S proteasome and blocked by phosphatidylinositol 3'-kinase inhibition. Mol. Cell. Biol., *20*: 1489–1496, 2000.

IGF-I Receptor-Induced Cell-Cell Adhesion of MCF-7 Breast Cancer Cells Requires the Expression of a Junction Protein ZO-1

Loredana Mauro[1, 2], Monica Bartucci[1, 2], Catia Morelli[1,2], Sebastiano Ando'[2], and Eva Surmacz[1]*

[1]Kimmel Cancer Center, Thomas Jefferson University, Philadelphia, PA 19107, [2]Department of Cellular Biology and Faculty of Pharmacy, University of Calabria, 87030 Rende (Cs) Italy

Running Title: IGF-IR upregulates adhesion through ZO-1

*Corresponding Author: Eva Surmacz, Ph.D.
Kimmel Cancer Center, Thomas Jefferson University
233 S 10th Street, BLSB 631, Philadelphia, Pa 19107
Tel.: 215-503-4512, Fax: 215-923-0249
e-mail: eva.surmacz@mail.tju.edu

SUMMARY

Hyperactivation of the insulin-like growth factor I receptor (IGF-IR) contributes to primary breast cancer development, but the role of the IGF-IR in tumor metastasis is unclear. Here we studied the effects of the IGF-IR on intercellular connections mediated by the major epithelial adhesion protein, E-cadherin (E-cad). We found that IGF-IR overexpression markedly stimulated aggregation in E-cad-positive MCF-7 breast cancer cells, but not in E-cad-negative MDA-MB-231 cells. However, when the IGF-IR and E-cad were co-expressed in MDA-MB-231 cells, cell-cell adhesion was substantially increased. The IGF-IR-dependent cell-cell adhesion of MCF-7 cells was not related to altered expression of E-cad, α-, β-, or γ-catenins, but coincided with the upregulation of another element of the E-cad complex, ZO-1. ZO-1 expression (mRNA and protein) was induced by IGF-I and was blocked in MCF-7 cells with a tyrosine kinase-defective IGF-IR mutant. By co-immunoprecipitation, we found that ZO-1 associates with the E-cad complex and the IGF-IR. High levels of ZO-1 coincided with an increased IGF-IR/α-catenin/ZO-1binding and improved ZO-1/actin association, while downregulation of ZO-1 by the expression of an anti-ZO-1 RNA inhibited IGF-IR-dependent cell-cell adhesion. The results suggested that one of the mechanisms by which the activated IGF-IR regulates E-cad-mediated cell-cell adhesion is overexpression of ZO-1 and resulting stronger connections between the E-cad complex and the actin cytoskeleton. We hypothesize that in E-cad-positive cells, the IGF-IR may produce anti-metastatic effects.

INTRODUCTION

The insulin-like growth factor I (IGF-I) receptor (IGF-IR) is a ubiquitous tyrosine kinase capable of regulating different growth-related and -unrelated processes (1-3).

Recent evidence indicates that the IGF-IR may be involved in breast cancer development. The IGF-IR is significantly (10-14-fold) overexpressed in estrogen receptor (ER)-positive primary breast tumors compared to normal mammary epithelium or benign tumors (1, 4). Moreover, the intrinsic ligand-independent tyrosine kinase activity of the IGF-IR has been found substantially upregulated (~2-4-fold) in breast cancer cells (4). It has been suggested that the increased receptor function coupled with enhanced receptor expression amounts to a 40-fold elevation in IGF-IR activity in ER-positive breast tumors (4). Recent clinical and experimental data indicate that upregulation of IGF-IR signaling in ER-positive breast cancer cells is associated with autonomous cell proliferation, estrogen-independence, and increased resistance to various anti-tumor treatments (1). Consequently, it is believed that hyperactivation of the IGF-IR may induce and sustain the growth of primary breast tumors (1).

The role of the IGF-IR in breast cancer metastasis, however, is unclear. The experimental data suggested that the IGF-IR has a function in cell spreading, as it effectively stimulates the motility of different metastatic breast cancer cell lines lacking the expression of a major adhesion protein E-cadherin (E-cad) (1, 5, 6). On the other hand, we and others have shown that in more differentiated E-cad-positive cells, IGF-I treatment or IGF-IR overexpression upregulates cell-cell adhesion, which correlates with increased cell survival in 3-dimensional (3-D) culture and reduced cell migration in vitro and in organ culture (1, 7-10).

The mechanism of IGF-I-dependent intercellular adhesion and the clinical consequences of this phenomenon have not been fully elucidated. Previously, we demonstrated that in MCF-7 human breast cancer cells, the IGF-IR co-localizes and co-

precipitates with the E-cad complex, and IGF-induced aggregation is blocked with an anti-E-cad antibody (7). In this study we assessed the effects of the IGF-IR on the elements of the E-cad adhesion complex, i.e. E-cad, β-, γ-, and α-catenins and α-catenin-associated proteins (see Fig. 6). The initial results prompted us to focus on an α-catenin-binding element—a junction protein *zonula occludens-1* (ZO-1).

ZO-1 is a ~220 kDa scaffolding protein containing various domains (an SH3 domain, three PDZ domains, a proline-rich region, and a guanylate kinase domain), which allow its interaction with specialized sites of plasma membrane as well as with other proteins (11, 12). ZO-1 is a characteristic element of tight junctions, but recently its presence has also been demonstrated in E-cad adherens junctions (13-15). The role of ZO-1 in adherens junctions is yet unclear, but it is assumed that it may functionally link E-cad with the actin cytoskeleton, as it associates with α-catenin and actin through its N- and C-terminus, respectively (13, see Fig. 6). In addition, as a member of the MAGUK (membrane-associated guanylate kinase homologues) family of putative signaling proteins, ZO-1 may be involved in signal transduction. Indeed, ZO-1 has been found to bind a target of Ras, AF6 (16). Deletions or mutations in the ZO-1 gene produced overgrowth, suggesting that ZO-1 may act as a tumor suppressor (11). In breast cancer, ZO-1 is usually co-expressed with E-cad and is a strong independent marker of a more differentiated phenotype (17).

At present, very little is known about the regulation of ZO-1 by growth factors. However, some recent studies demonstrated that EGF (epidermal growth factor) and VEGF (vascular endothelial growth factor) are able to increase ZO-1 tyrosine phosphorylation, modulate its subcellular localization, and consequently produce increased

permeability (18-20). Here, we present the first evidence that in MCF-7 breast cancer cells 1) the IGF-IR upregulates ZO-1 expression; 2) elevated levels of ZO-1 coincide with enhanced IGF-IR/E-cad-mediated cell-cell adhesion; and 3) ZO-1 expression is required for IGF-IR-increased cell aggregation in E-cad-positive MCF-7 cells.

MATERIALS AND METHODS

Expression Plasmids. E-cad expression plasmid. The pBAT-EM2 plasmid is a derivative of pBR322 and contains the mouse E-cad cDNA cloned under the β-actin promoter in pBR322 (21). As demonstrated previously, transfection of MDA-MB-231cells with pBAT-EM2 results in E-cad overexpression, improved cell aggregation, and reduced metastatic potential of the cells (21, 22).

Antisense ZO-1 RNA vector. The pcDNA3/anti-ZO-1 plasmid encoding the anti-ZO-1 antisense RNA contains a 959 bp BamH1 fragment of the human ZO-1 cDNA (nt 4205-5164) inserted (in the 3'-5' orientation) into the pcDNA3.1/Hygro plasmid (Invitrogen). PcDNA3/sense-ZO-1 is the control vector in which the above 959 bp ZO-1 cDNA fragment was cloned in the 5'-3' orientation.

Cell Lines and Cell Culture Conditions. MCF-7/IGF-IR, clone 12, 15 and 17 are MCF-7-derived clones overexpressing the IGF-IR at the levels $5x10^5$, $3x10^6$, and $1x10^6$ receptors/cell, respectively (7). To avoid clonal variation, in several experiments we used a population of mixed clones 12, 15 and 17. The mixed population is referred to as MCF-7/IGF-IR cells and expresses ~ $0.9x10^6$ IGF-IR receptors/cell (which represents ~18-fold overexpression over the levels in normal cells)(1). MCF-7/IGF-IR/Y3F express an IGF-IR (~$3x10^6$ receptors/cell) with inactivating mutations in the tyrosine kinase domain (Tyr

1131, 1135, 1136 replaced with Phe) (23). MCF-7/IGF-IR/Y3F cells were derived from MCF-7 cells by stable transfection with the pcDNA3/IGF-IR/KR plasmid and subsequent selection in 2 mg/ml G418. The results obtained with the MCF-7/IGF-IR/Y3F clone were verified using a population of MCF-7 cells transiently transfected with the IGF-IR/Y3F vector (see below). MCF-7/IGF-IR/anti-ZO-1 and MCF-7/IGF-IR/sense-ZO-1 cells were derived from MCF-7/IGF-IR clone 15 by stable transfection with the antisense- and sense-ZO-1 vectors, respectively, and subsequent selection in 500 μg/ml Hygromycin B.

MDA-MB-231 is a metastatic breast cancer cell line lacking E-cad and expressing ~ $7x10^3$ IGF-IR receptors/cell (24, Bartucci et al., in revision). MDA-MB-231/IGF-IR clone 31 was derived from MDA-MB-231 cells by stable transfection with the pcDNA3/IGF-IR plasmid. MDA-MB-231/IGF-IR cells express ~ 250,000 IGF-IR/cell (Bartucci et al., in revision).

All cell lines were grown in DMEM:F12 (1:1) containing 5% calf serum (CS). MCF-7- and MDA-MB-231-derived clones transfected with the wild type or mutant IGF-IR were maintained in growth medium with 100 μg/ml G418. MCF-7/IGF-IR/anti-ZO-1 and MCF-7/IGF-IR/sense-ZO-1 cells were cultured in growth medium with 50 μg/ml Hygromycin B. In the experiments requiring serum-free conditions, the cells were cultured in phenol red-free DMEM containing 0.5 mg/ml BSA, 1 uM FeSO4 and 2 mM L-glutamine (referred to as SFM).

Transient Transfection. MDA-MB-231 and MDA-MB-231/IGF-IR cells were transiently transfected using Lipofectamine 2000 (Gibco) (reagent/DNA ratio = 5 μl/1μg). The transfection was carried out in growth medium for 24 h, then, the cells were lysed and processed for E-cad Western blotting (WB). To evaluate the extent of cell-cell adhesion in

the transfected MDA-MB-231 and MDA-MB-231/IGF-IR cells, the cells were trypsinized upon transfection, counted and placed in 3-D suspension culture, as described below. MCF-7 cells were transfected for 6 h in growth medium using Fugene 6 (Roche) (reagent/DNA ratio = 3 μl/1μg). To study IGF-I signaling, the transfected MCF-7 cells were shifted to SFM for 36 h and stimulated with IGF-I for 15 min. The efficiency of transfection (transfected cells/total cell number) was at least 70% for all cell types, and was estimated by scoring fluorescent cells in cultures transfected with the plasmid pCMS (encoding Green Fluorescent Protein) (Invitrogen).

3-D Spheroid Culture. The cells were grown to 70-80% confluence, trypsinized, and plated as single cell suspension in 2%-agar-coated plates containing either normal growth medium or SFM. $2x10^6$ cells were plated per 100 mm culture dish. To generate 3-D spheroids, the plates were rotated for 4 h at 37°C. The spheroids started to assemble at ~1 h after plating and were completely organized after 3-4 h of culture in suspension. The 3-D cultures were photographed using a phase contrast microscope (Nikon or Olympus). The extent of aggregation was scored by measuring the spheroids with an ocular micrometer. For each cell type, the spheroids of 25≤50, 50≤100, and >100 μm (in the smallest cross-section) were counted in 10 different fields under 10x magnification.

IGF Stimulation. 70% confluent cell cultures were synchronized in SFM for 36 h and then stimulated with 20 ng/ml IGF-I for 0-72 h.

Immunoprecipitation and Western Blotting. The expression of different elements of the adhesion complex was assessed in 500 μg of protein lysate by immunoprecipitation (IP) and Western blotting (WB) with appropriate antibodies. The expression of ERK1/ERK2 was tested in 50 μg of total cell lysate. The cell lysis buffer contained 50

mM HEPES pH 7.5, 150 mM NaCl, 1% Triton X-100, 1.5 mM $MgCl_2$, 1 mM $CaCl_2$, 100 mM NaF, 0.2 mM Na_3VO_4, 1% PMSF, 1% aprotinin, as described before (25). The following antibodies were used: anti-ZO-1 polyclonal antibody (pAb) (Zymed Laboratories) for ZO-1 IP (5 μg/ml) and WB (2 μg/ml); anti-E-cad monoclonal antibody (mAB), clone 36 (Transduction Laboratories) for E-cadherin IP (2 μg/ml) and WB (0.1 μg/ml); anti-α-catenin pAb (Sigma or Zymed Laboratories) for α-catenin IP (4 μg/ml) and WB (anti-serum dilution 1:4,000); anti-β-catenin mAb (Transduction Laboratories) for β-catenin IP (4 μg/ml) and WB (0.5 μg/ml); anti-γ catenin pAb (Sigma) for γ-catenin WB (1 μg/ml); anti-actin mAb clone AC-40 (Sigma) for actin WB (0.4 μg/ml); anti-IGF-IR mAb, clone alpha IR-3 (Calbiochem) for IGF-IR IP (3 μg/ml), and anti-IGF-IR pAb C-20 (Santa Cruz) for IGF-IR WB (0.2 μg/ml); anti-p85 pAb (UBI) for p85 subunit of PI-3 kinase WB (0.25 μg/ml); anti-phospho-MAPK mAb (New England Biolabs) for active ERK1/ERK2 WB (0.5 μg/ml); anti-MAPK pAb (New England Biolabs) for total ERK1/ERK2 WB (1 μg/ml). Tyrosine phosphorylation of immunoprecipitated proteins was measured by WB with anti-phosphotyrosine mAb (Transduction Laboratories) (0.03 μg/ml). WBs were developed using an ECL chemiluminescence kit (Amersham). The intensity of bands representing relevant proteins was measured by laser densitometry scanning.

RESULTS

IGF-IR overexpression stimulates cell-cell adhesion through E-cad-dependent mechanism. First, we demonstrated that under 3-D culture conditions, overexpression of the IGF-IR stimulated cell-cell adhesion in E-cad-positive MCF-7 breast cancer cells, but

not in E-cad-negative MDA-MB-231 cells (Fig. 1 A, B, and Tab. 1). However, co-expression of the IGF-IR and E-cad resulted in robust cell-cell adhesion of MDA-MB-231 cells, while the expression of E-cad alone was less efficient in inducing intercellular contacts (Fig. 1 C, D, and Tab. 1). These results together with our previous data that IGF-IR-mediated aggregation in MCF-7 cells is blocked with an anti-E-cad antibody (7) indicated that IGF-IR adhesion signals are transmitted through the E-cad complex.

IGF-IR overexpression upregulates ZO-1. We tested whether high levels of the IGF-IR affect the expression of the proteins within the E-cad complex. We found that in MCF-7 and MCF-7/IGF-IR cells cultured as 3-D spheroids, the levels of E-cad, α-, β-, and γ-catenin were similar, however, the abundance of ZO-1 was significantly increased in MCF-7/IGF-IR cells (Fig. 2). The tyrosine phosphorylation of all these adhesion proteins was undetectable in spheroids, and was not influenced by IGF-IR overexpression (Fig. 5 and data not shown).

To investigate whether the increased expression of ZO-1 in MCF-7/IGF-IR cells depends on IGF-IR tyrosine kinase activity, we generated by stable or transient transfection MCF-7/IGF-IR/Y3F cells expressing high levels of a kinase-defective IGF-IR mutant (IGF-IR/Y3F). The overexpression of the IGF-IR/Y3F mutant resulted in impaired IGF-I response, which was reflected by markedly reduced IGF-IR and IRS-1 tyrosine phosphorylation, decreased IRS-1/p85 binding, and diminished ERK1/ERK2 stimulation (Fig. 3). The basal expression of ZO-1 in MCF-7/IGF-IR/Y3F cells was significantly reduced compared to that in MCF-7/IGF-IR cells, indicating that tyrosine kinase activity of the IGF-IR is required for the upregulation of ZO-1 (Fig. 3). Interestingly, the inhibition of IGF-I response did not affect E-cad expression, suggesting a selective action of the

IGF-IR towards ZO-1 (Fig. 3). The blockade of the IGF-IR signal in MCF-7/IGF-IR/Y3F cells coincided with reduced cell-cell adhesion (Tab. 1).

ZO-1 mRNA and protein expression is regulated by IGF-I. To establish whether the activation of the IGF-IR by IGF produces a similar effect on ZO-1 as that seen with IGF-IR overexpression, we studied ZO-1 mRNA and protein in MCF-7 and MCF-7/IGF-IR cells treated with 20 ng/ml IGF-I for 1-72h (Fig. 4). In MCF-7 cells cultured in SFM, the basal levels of ZO-1 mRNA were low, and were markedly increased between 4 and 36h of IGF-I treatment (Fig. 4A). In contrast, the abundance of ZO-1 mRNA was always elevated in MCF-7/IGF-IR cells, and was only moderately improved by IGF-I (4-72 h) (Fig. 4A). ZO-1 protein levels in IGF-I-treated cells generally reflected the expression of ZO-1 mRNA (Fig. 4B).

Interactions of ZO-1 with the E-cad complex in MCF-7/IGF-IR cells. It has been recently reported that ZO-1 is an element of the E-cad complex (12-14). This complex also contains the IGF-IR, as described in our previous work (7, 8). Here, we analyzed tyrosine phosphorylation status of the IGF-IR, E-cad, and ZO-1, and the interactions among these proteins in MCF-7 and MCF-7/IGF-IR cells cultured as 3-D spheroids (Fig. 5). The autophosphorylation of the IGF-IR was elevated in MCF-7/IGF-IR cells, reflecting the increased responsiveness of the cells to IGF-IR ligands (IGF-I, IGF-II, and insulin) present in serum. However, tyrosine phosphorylation of E-cad and ZO-1 were unaffected by IGF-IR overexpression (Fig. 5A). Similarly, high levels of the IGF-IR did not affect tyrosine phosphorylation of α-, β-, or γ-catenin (data not shown). Next, we asked whether hyperactivation of the IGF-IR and increased expression ZO-1 have consequences on the associations among the proteins within the E-cad complex. Co-

immunoprecipitation experiments demonstrated that IGF-IR overexpression resulted in an increased abundance of IGF-IR/E-cad and IGF-IR/ZO-1 complexes (Fig. 5A). Also, the elevated levels of ZO-1 in MCF-7/IGF-IR cells coincided with an increased association of ZO-1 with either E-cad or the IGF-IR (Fig. 5A). Moreover, the binding of α-catenin (an ZO-1-associated protein) to the IGF-IR or ZO-1, but not to E-cad, was greater in MCF-7/IGF-IR cells than in MCF-7 cells (Fig. 5A). The presence of α-catenin in IGF-IR immunoprecipitates was confirmed with cell lysates in which α-catenin was first removed with a specific antibody. As expected, immunoprecipitation of such depleted lysates with either anti-IGF-IR or anti-E-cad antibodies revealed reduced α-catenin/E-cad and α-catenin/IGF-IR associations (Fig. 5B). Further experiments with α-catenin immunoprecipitates indicated increased abundance of α-catenin/actin and α-catenin/ZO-1 complexes in MCF-7/IGF-IR cells (Fig. 5C). A hypothetical model of possible interactions between adhesion proteins and the IGF-IR is shown in Fig. 6.

Downregulation of ZO-1 results in decreased cell-cell adhesion in MCF-7/IGF-IR cells. Since the results suggested that ZO-1 may be an important intermediate in IGF-IR-stimulated cell-cell adhesion, we set out to confirm this notion using MCF-7/IGF-IR cells in which ZO-1 levels were downregulated by the expression of an anti-ZO-1 RNA (MCF-7/IGF-IR/anti-ZO-1 cells) (Fig. 7). The clones with the best ZO-1 reduction and an intact E-cad and IGF-IR expression were analyzed in 3-D culture. The cell-cell adhesion of MCF-7/IGF-IR/anti-ZO-1 cells was greatly inhibited compared with that in the parental MCF-7/IGF-IR cells (Fig. 7 and Tab. 1). The expression of the anti-ZO-1 plasmid in the parental MCF-7 cells was toxic and no viable clones were obtained. The transfection of the sense-ZO-1 vector had no effect on cell-cell adhesion (data not shown).

DISCUSSION

Cell-cell adhesion is a known factor modulating the motility of tumor cells, and consequently, impacting tumor metastasis (26). The regulation of this process by exogenous growth factors is still not well understood. In E-cad-positive breast cancer cells, the overexpression or activation of the IGF-IR has been shown to stimulate cell-cell adhesion and reduce cell spreading in vitro or in organ culture (7-10). The IGF-IR has also been found co-localized and co-precipitated with the E-cad adhesion complex (7, 8). The mechanism of IGF-IR-stimulated E-cad-dependent cell-cell adhesion is unknown and has been investigated in this work. We found that 1) IGF-IR overexpression increased aggregation in E-cad-positive cells, but not in E-cad-negative cells; 2) high expression of both IGF-IR and E-cad markedly improved cell aggregation in E-cad-negative cells; 3) IGF-IR-dependent cell-cell adhesion in E-cad-positive cells did not affect the expression of E-cad, α-, β-, or γ-catenins, but coincided with upregulation of ZO-1; 4) ZO-1 expression was induced by IGF-I and required IGF-IR tyrosine kinase activity; 5) high levels of ZO-1 coincided with an increased IGF-IR/α-catenin/ZO-1 binding and improved ZO-1/actin association, while downregulation of ZO-1 by the expression of an anti-ZO-1 RNA inhibited IGF-IR-dependent cell-cell adhesion. We hypothesize that the mechanism, or one of the mechanisms, by which the activated IGF-IR stimulates cell-cell adhesion is overexpression of ZO-1 and resultant stronger connections between the E-cad complex and the actin cytoskeleton.

Very little is known about the regulation of ZO-1 by growth factors. Several growth factors (EGF, VEGF) have been demonstrated to increase tyrosine

phosphorylation of ZO-1 in different cellular model systems (18, 19). Hyperphosphorylation of ZO-1 usually coincides with its departure from tight junctions into the cytoplasm and with increased permeability (18, 19). In addition, v-src-increased ZO-1 tyrosine phosphorylation has been linked with decreased cell-cell adhesion (27). IGF-I, on the other hand, has been shown to stabilize ZO-1 in tight junctions and to preserve epithelial barrier in embryonic kidney cells and in pig thyrocytes (28, 29). However, the effects of IGF-I on ZO-1 expression and function in breast cancer cells have never been explored. Our findings provide the first evidence that the activation of the IGF-IR upregulates ZO-1 mRNA and protein levels, without affecting ZO-1 tyrosine phosphorylation. Consistent with the results obtained in other models, we noted increased adhesion in cells overexpressing ZO-1 and reduced aggregation in cells with downregulated ZO-1 levels.

IGF-IR tyrosine phosphorylation was required for the stimulation of ZO-1 expression, as the basal levels of ZO-1 were not increased in MCF-7/IGF-IR/Y3F cells expressing a dominant-negative kinase-defective mutant of the IGF-IR. However, the putative IGF-I signaling pathways leading to ZO-1 expression have yet to be characterized. Our preliminary data with MCF-7/IRS-1 cells, in which the major IGF-IR/IRS-1/PI-3K growth/survival pathway is hyperactivated, suggested that this pathway is not involved in ZO-1 regulation (Surmacz et al., data not shown).

The clinical implications of IGF-induced and ZO-1-mediated cell-cell adhesion on tumor development and progression are unknown. Until now, the data from our and other laboratories suggest that in E-cad-positive breast cancer cells, IGF-IR improves cell-cell adhesion and cell survival in 3-D culture, but at the same, reduces cell spreading (1). Thus,

one consequence of IGF-IR overexpression in breast cancer could be increased growth and survival of the primary tumor, but reduced cell metastasis. This hypothesis is consistent with the observation that the IGF-IR is a good prognostic indicator for breast cancer, as tumors with good prognosis express much higher levels of the IGF-IR than tumors with bad prognosis (1, 30, 31). Notably, independent study has shown that in breast tumors, E-cad and ZO-1 are co-expressed and are markers of a more differentiated phenotype (17). A formal analysis of the correlations between ZO-1 and the IGF-IR is underway in our laboratory and should help in clarifying the role of the IGF-IR in breast cancer progression.

ACKNOWLEDGMENTS

Drs. J. M. Anderson and A. S. Fanning (Yale University, New Haven, CT) generously provided the pSKZO-1 plasmid encoding the human ZO-1 cDNA. The E-cad expression vector pBAT-EM2 was a gift form Drs. M. Takeichi (Kyoto University, Kyoto, Japan) and T. Yoneda (University of Texas, San Antonio, TX). The MCF-7/Y3F clone was developed by Dr. M. Guvakova (University of Pennsylvania, Philadelphia, PA). This work was supported by the following grants and awards: U.S. Department of Defense DAMD17-99-1-9407 and DAMD17-97-1-7211; International Union against Cancer Award ICRETT 1007/1999, and POP 98 grant from Regione Calabria.

REFERENCES

1. Surmacz, E. (2000) J. Mammary Gland Biol. Neopl. **5,** 95-105

2. Werner, H., and Le Roith, D. (2000) Cell. Mol. Life Sci. **57,** 932-42

3. Baserga, R. (1999) Exp. Cell Res. **253,** 1-6

4. Resnik, J. L., Reichart, D. B., Huey, K., Webster, N. J. G., and Seely, B. L. (1998) Cancer Res. **58,** 1159-1164

5. Dunn, S. E., Ehrlich, M., Sharp, N. J. H., Reiss, K., Solomon, G., Hawkins, R., Baserga, R., and Barrett, J. C. (1998) Cancer Res. **58,** 3353-3361

6. Doerr, M., and Jones, J. J. (1996) Biol. Chem. **271**, 2443-2447

7. Guvakova, M. A., and Surmacz, E. (1997) Exp. Cell Res. **231,** 149-162

8. Surmacz, E., Guvakova, M., Nolan, M., Nicosia, R., and Sciacca, L. (1998) Breast Cancer Res. Treat. **47**, 255-267

9. Bracke, M. E., Vyncke B. M., Bruyneel, E.A., Vermeulen, S.J., De Bruyne, G. K., Van Larebeke, N. A., Vleminckx, K., Van Roy F.M., and Mareel, M.M. (1993) Br. J. Cancer **68,** 282-289

10. Bracke, M.E., Van Roy, F.M., and Mareel, M.M. (1996) Curr. Top. Microbiol. Immunol. **213,** 123-61

11. Willott, E., Balda, M. S., Fanning, A. S., Jameson, B., Van Itallie, C, and Anderson, J. M. (1993) Proc. Natl. Acad. Sci. USA **90**, 7834-7838

12. Tsukita, S., Furuse, M.,and Itoh, M. (1997) Soc. Gen. Phys. Series **52**, 69-76

13. Itoh, M., Nagafuchi, A., Moroi, S., and Tsukita, S. J. (1997) Cell Biol. **138,** 181-192

14. Rajasekaran, A.K., Hojo, M., Huima, T., and Rodriguez-Boulan, E. J. (1996) Cell Biol. **132,** 451-463

15. Provost, E., and Rimm DL (1999) Curr. Opin. Cell Biol. **11,** 567-72

16. Yamamoto, T., Harada, N., Kano, K., Taya, S., Canaani, E., Matsuura, Y., Mizoguchi, A., Ide, C., and Kaibuchi, K. J. (1997) Cell Biol. **139,** 785-795

17. Hoover, K. B., Liao, S-Y., and Bryant, P. J. (1998) Amer. J. Pathol. **153,** 1767-17773

18. Van Itallie, C. M., Balda, M. S. and Anderson, J. M. (1995) J. Cell Sci. **108,** 1735-1742

19. Antonetti, D.A., Barber, A.J., Hollinger, L.A., Wolpert, E.B., and Gardner, T.W. (1999) J. Biol. Chem . **274,** 23463-23467

20. Merwin, J.R., Anderson, J.M., Kocher, O., Van Itallie, C.M., and Madri, J.A. (1990) J. Cell. Physiol. **142,** 117-28

21. Nagafuchi, A., Shirayoshi, Y., Okazaki, K., Yasuda, K., and Takeichi, M. (1987) Nature **329,** 341-3

22. Mbalaviele, G., Dunstan, C.R., Sasaki, A., Williams, P.J., Mundy, G.R., and Yoneda, T. (1996) Cancer Res. **56**, 4063-70

23. Kato, H., Faria, T., Stannard, B., Roberts, C. T., Jr., and LeRoith, D. (1994) Mol. Endocrin. **8,** 40-50

24. Peyrat, J. P., Bonneterre, J., Dusanter-Fourt, I., Leroy-Martin, B., Dijane, J., and Demaille, A. (1989) Bull. Cancer **76,** 311-309

25. Mauro, L., Sisci, D., Salerno, M., Kim, J., Tam, T., Guvakova, M., Ando, S., and Surmacz, E. (1999) Exp. Cell Res. **252**, 439-448

26. Christofori, G., and Semb, H. (1999) Trends Biochem. Sci. **24,** 73-6

27. Takeda, H., Nagafuchi, A., Yonemura, S., Tsukita, S., Behrens, J., Birchmeier, W., and Tsukita, S. (1995) J. Cell Biol. **131,** 1839-1847

28. Sakurai, H., Barros, E.J., Tsukamoto, T., Barasch, J., Nigam, S.K. (1997) Proc. Natl. Acad. Sci. USA **94,** 6279-84

29. Ericson, L.E., and Nilsson, M. (1996) Eur. J. Endocrinol . **135,** 118-27

30. Pezzino, V., Papa, V., Milazzo, G., Gliozzo, B., Russo, P., and Scalia, P. L. (1996) Ann. NY Acad. Sci. **784,** 189-201

31. Schnarr, B., Strunz, K., Ohsam, J., Benner, A., Wacker, J., and Mayer, D. (2000) Int. J. Cancer **89**, 506-513

FIGURE LEGENDS

Fig. 1. IGF-IR overexpression stimulates cell-cell adhesion in E-cad-positive but not in E-cad-negative breast cancer cells. A) E-cad-positive MCF-7 and MCF-7/IGF-IR cells and E-cad-negative MDA-MB-231 and MDA-MB-231/IGF-IR cells were cultured in normal growth medium as 3-D spheroids for 24 h, as described in Materials and Methods, and then photographed under phase contrast. a) MCF-7 cells expressing ~ $6x10^4$ IGF-IR/cell/cell (7); b) MCF-7/IGF-IR, clone 12 expressing ~$5x10^5$ IGF-IGF-IR/cell (7); c) MDA-MB-231 cells with ~$7x10^3$ IGF-IGF-IR/cell (24), and d) MDA-MB-231/IGF-IR, clone 31 with ~ $3x10^5$ IGF-IR/cell (Bartucci et al., in revision). The bar in a) equals 50 μm. **B)** IGF-IR levels in cells pictured in Fig. 1 A, a-d were assessed by WB in 50 μg of cell lysate, as described in Materials and Methods. **C)** MDA-MB-231 and MDA-MB-231/IGF-IR cells were transiently transfected with the E-cad expression plasmid (b and d) or a vector alone (a and c) and then cultured in suspension as 3-D spheroids. The bar in a) equals 100 μm. **D)** E-cad levels in cells pictured in Fig. 1 C, a-d were determined by WB in 50 μg of cell lysate, as described in Materials and Methods.

Fig. 2. Expression of adhesion proteins in MCF-7 and MCF-7/IGF-IR cells. The expression of adhesion proteins and the IGF-IR was studied in 50 μg of protein lysates

obtained from cells cultured as 3-D spheroids in normal growth medium. MCF-7/IGF-IR cells are pooled MCF-7/IGF-IR clones 12, 15, and 17 (Materials and Methods). **A)** The levels of the IGF-IR, E-cad, α-, β-, γ-catenin, and ZO-1 detected by WB using specific Abs (Materials and Methods). **B)** The expression of ZO-1 in MCF-7 cells and in MCF-7/IGF-IR clones 12, 17, and 15, expressing ~ $5x10^5$, $1x10^6$, and $3x10^6$ IGF-IR/cell, respectively (7).

Fig. 3. ZO-1 expression is inhibited in MCF-7/IGF-IR/Y3F cells. MCF-7/IGF-IR cells expressing the wild-type IGF-IR (WT) and MCF-7 IGF-IR/Y3F cells stably transfected with a dominant-negative kinase-defective IGF-IR mutant (Y3F) were synchronized in SFM for 36 h and then stimulated for 15 min with 20 ng/ml IGF-I, as described in Materials and Methods. The expression and tyrosine phosphorylation (PY) of the IGF-IR and IRS-1 in the cells were detected by IP and WB in 500 μg of protein lysates. The binding of p85 subunit of PI-3 kinase to IRS-1 (IRS-1/p85) was studied by WB in IRS-1 IPs. The expression of active ERK1/ERK2 (p-ERK1/2), total ERK1/2, ZO-1 and E-cad was evaluated by WB in 50 μg of total protein lysates. The specific Abs used are listed in Materials and Methods. Similar results were obtained with MCF-7 cells transiently transfected with the IGF-IR/Y3F expression vector.

Fig. 4. ZO-1 mRNA and protein are regulated by IGF-I. A) MCF-7 cells and MCF-7/IGF-IR were synchronized in SFM (time 0) and then stimulated with 20 ng/ml IGF-I for different times (1-72 h). The expression of 7.8 kb ZO-1 mRNA in MCF-7 and MCF-7/IGF-IR cells was studied by Northern blotting in 20 μg of total RNA using a ^{32}P-dCTP-

labeled ZO-1 probe (described in Materials and Methods). 28 and 18 S rRNA are shown as a control of RNA loading. **B)** The expression of ZO-1 protein in IGF-I- treated cells was detected by WB as described under Fig. 3.

Fig. 5. Interactions of ZO-1 with the IGF-IR in the E-cad complex. A) The IGF-IR, E-cad, and ZO-1 were immunoprecipitated (IP) from 500 μg of total protein lysates obtained from MCF-7 and MCF-7/IGF-IR cells cultured as 3-D spheroids in normal growth medium. The IPs were then probed by WB for phosphotyrosine (PY), the IGF-IR (~97 kDa) , ZO-1 (~220 kDa), E-cad (~ 120 kDa), and α-catenin (~102 kDa). **B)** To confirm α-catenin presence in IGF-IR immunoprecipitates, the lysates were first treated with anti-α-catenin Ab (Zymed) O/N to deplete α-catenin, and then immunoprecipitated with either anti-E-cad or anti-IGF-IR Abs. The E-cad and IGF-IR IPs were then probed with another anti-α-catenin Ab (Sigma). Note significantly reduced α-catenin associations with IGF-IR and E-cad compared with that seen in A). **C)** 500 μg of protein lysates were precipitated with anti-α-catenin Ab and probed by WB for α-catenin, actin, and ZO-1. The blots presented in **A, B,** and **C** were identically developed with film exposure time 10 sec.

Fig. 6. Possible interactions between ZO-1 and the IGF-IR within the E-cad complex. The well established connections between E-cad, catenins and actin are shown as solid lines. The proposed connections between the IGF-IR , α-catenin, ZO-1, and actin

are drown as broken lines. At present, it is not known whether the IGF-IR interacts with α-catenin directly, or other intermediate proteins are involved.

Fig. 7. Reduced cell-cell adhesion in MCF-7/IGF-IR/anti-ZO-1 cells. MCF-7/IGF-IR/anti-ZO-1 clones were obtained by stable transfection of MCF-7/IGF-IR cells with an anti-ZO-1 RNA expression plasmid (Materials and Methods). The levels of ZO-1, IGF-IR, and E-cad in the parental MCF-7/IGF-IR cells (A) and in the clones (B and C) were studied by WB in 50 μg of protein lysate. The aggregation of cells was studied in 3-D culture, as described in Materials and Methods. The bar in B) represents 50 μm.

TABLES

TABLE 1. Effects of IGF-IR and ZO-1 expression on cell aggregation in E-cad-positive and -negative breast cancer cells.

Cells	*Spheroids*		
	25 ≤ 50 μm	**50 ≤ 100 μm**	**> 100 μm**
MCF-7	21.0±1.9	96.0±6.7	2.7±0.9
MCF-7/IGF-IR	1.7±0.7	22.3±1.4	86.5±3.9
MCF-7/IGF-IR/anti-ZO-1	75.0±3.5	40.7±2.1	0.0±0.0
MCF-7/Y3F	45.0±2.9	39.8±4.6	0.0±0.0
MDA-MB-231	7.0±0.6	0.5±0.2	0.0±0.0
MDA-MB-231/IGF-IR	12.5±0.8	0.5±0.1	0.0±0.0
MDA-MB-231/E-cad	39.8±3.6	15.2±1.1	0.0±0.0
MDA-MB-231/vector	10.0±1.4	0.6±0.4	0.0±0.0
MDA-MB-231/IGF-IR/E-cad	27.0±2.2	68.3±7.2	8.0±1.5
MDA-MB-231/IGF-IR/vector	18.6±2.2	0.9±0.3	0.0±0.0

The stable cell lines (MCF-7, MCF-7/IGF-IR, MCF-7/IGF-IR/anti-ZO-1, MCF-7/Y3F, MDA-MB-231, and MDA-MB-231/IGF-IR) and transiently transfected populations (MDA-MB-231/E-cad, MDA-MB-231/vector, MDA-MB-231/IGF-IR/E-cad, and MDA-MB-231/IGF-IR/vector) were cultured as 3-D spheroids in normal growth medium. The number of spheroids of different sizes was established as described in Materials and Methods. The values represent a sum of spheroids in 10 optical fields under 10x magnification. The results are average ±SE from at least 3 experiments. Representative 3-D cultures are shown in Fig. 1 and 7.

Fig. 1

Fig. 1

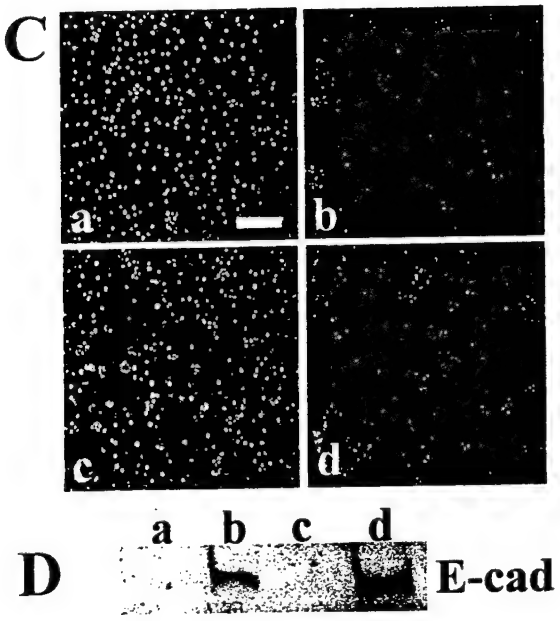

Fig. 2

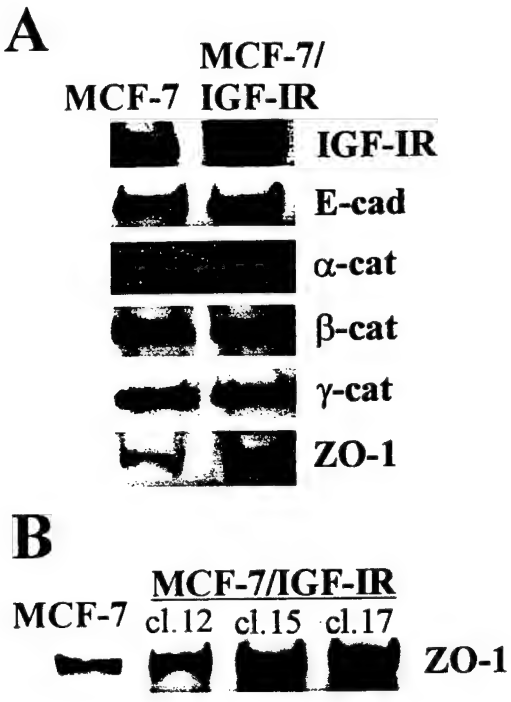
A
MCF-7
MCF-7/
IGF-IR
IGF-IR
E-cad
α-cat
β-cat
γ-cat
ZO-1
B
MCF-7/IGF-IR
MCF-7
cl.12
cl.15
cl.17
ZO-1

Fig. 3

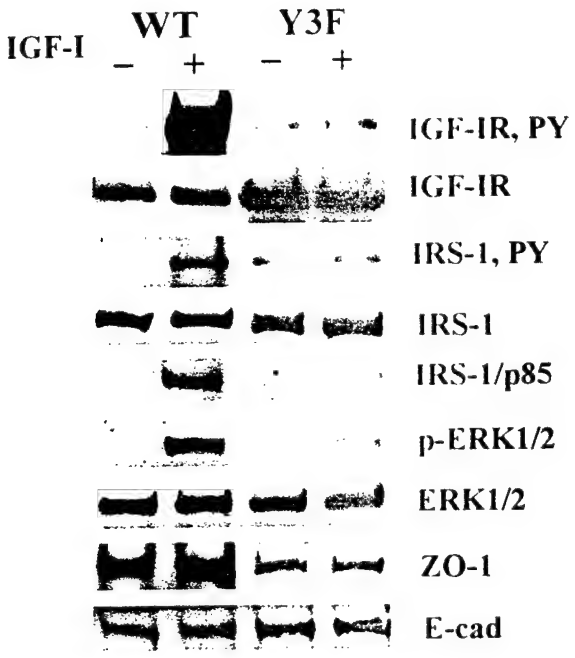
IGF-I
WT
Y3F
–
+
–
+
IGF-IR, PY
IGF-IR
IRS-1, PY
IRS-1
IRS-1/p85
p-ERK1/2
ERK1/2
ZO-1
E-cad

Fig. 4

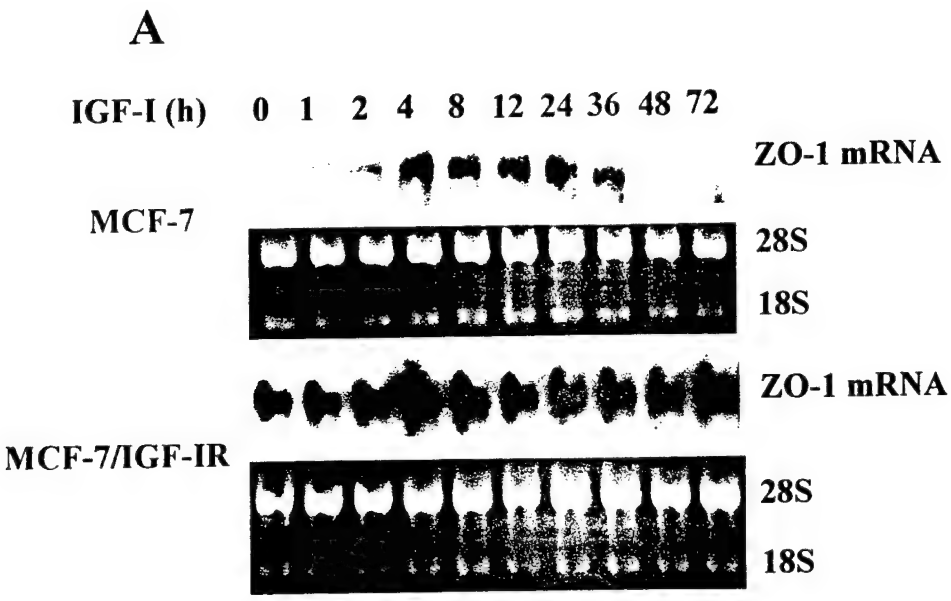
A
IGF-I (h) 0 1 2 4 8 12 24 36 48 72
ZO-1 mRNA
MCF-7
28S
18S
ZO-1 mRNA
MCF-7/IGF-IR
28S
18S

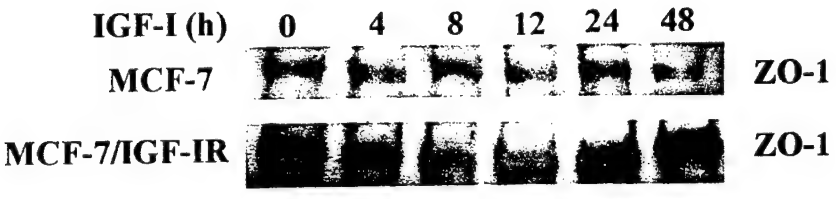
B
IGF-I (h) 0 4 8 12 24 48
MCF-7
ZO-1
MCF-7/IGF-IR
ZO-1

Fig. 5

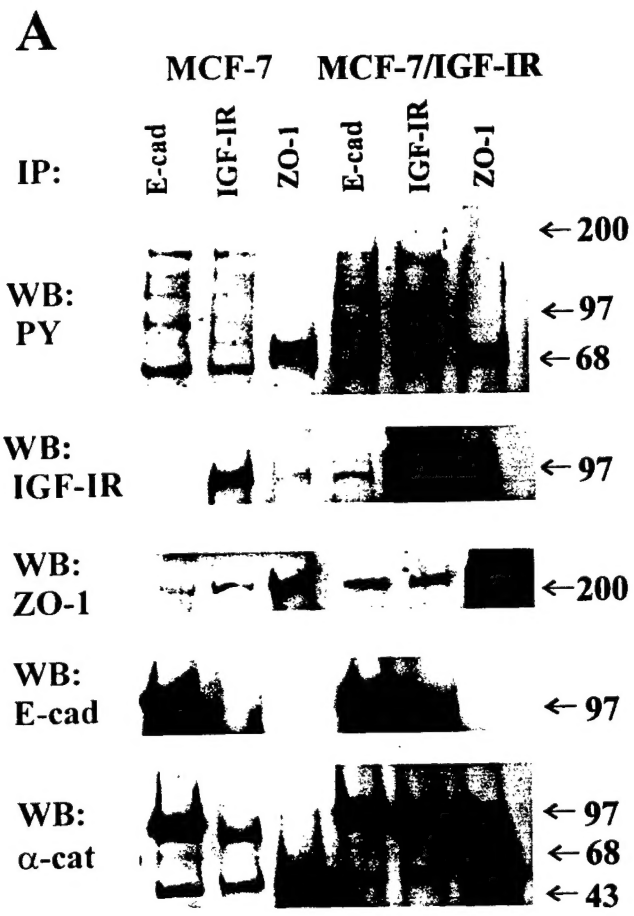
A
MCF-7
MCF-7/IGF-IR
IP:
E-cad
IGF-IR
ZO-1
E-cad
IGF-IR
ZO-1
WB:
PY
←200
←97
←68
WB:
IGF-IR
←97
WB:
ZO-1
←200
WB:
E-cad
←97
WB:
α-cat
←97
←68
←43

Fig. 5

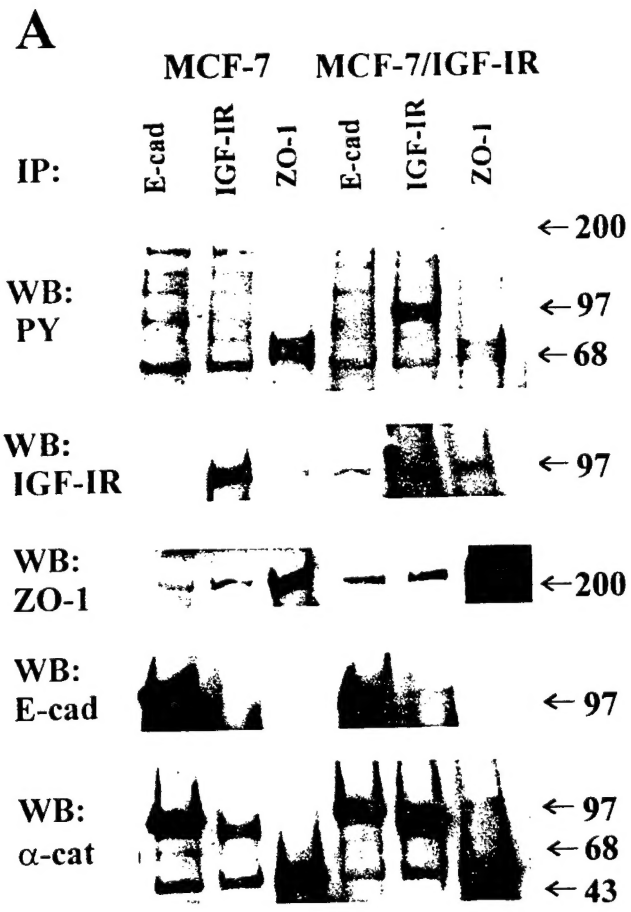
A
MCF-7
MCF-7/IGF-IR
IP:
E-cad
IGF-IR
ZO-1
E-cad
IGF-IR
ZO-1
WB: PY
WB: IGF-IR
WB: ZO-1
WB: E-cad
WB: α-cat
←200
←97
←68
←97
←200
←97
←97
←68
←43

Fig. 6

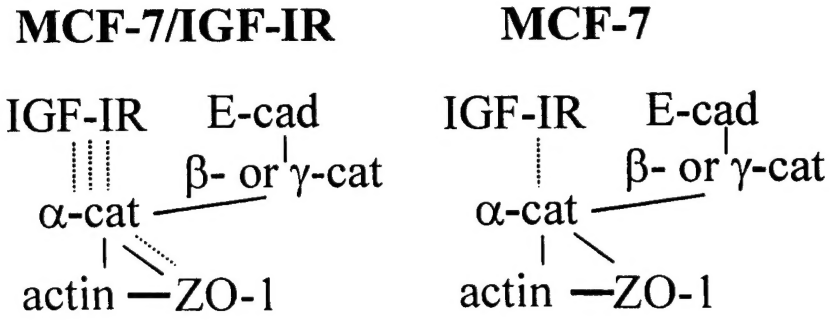
MCF-7/IGF-IR
IGF-IR
E-cad
β- or γ-cat
α-cat
actin
ZO-1
MCF-7
IGF-IR
E-cad
β- or γ-cat
α-cat
actin
ZO-1

Fig. 7